



Published in final edited form as:

Nat Rev Immunol. 2022 September ; 22(9): 550–566. doi:10.1038/s41577-022-00679-3.

The role of chromatin loop extrusion in antibody diversification

Yu Zhang^{1,†}, Xuefei Zhang^{2,3,4}, Hai-Qiang Dai^{2,3,5}, Hongli Hu², Frederick W. Alt^{2,†}

¹Center for Immunobiology, Department of Investigative Medicine, Western Michigan University Homer Stryker M.D. School of Medicine, Kalamazoo, MI, USA.

²Howard Hughes Medical Institute, Program in Cellular and Molecular Medicine, Boston Children's Hospital, Boston, MA, USA.

³Department of Genetics, Harvard Medical School, Boston, MA, USA.

⁴Present address: Biomedical Pioneering Innovation Center (BIOPIIC), Beijing Advanced Innovation Center for Genomics (ICG), Peking University, Beijing, China.

⁵Present address: Center for Excellence in Molecular Cell Science, Chinese Academy of Sciences, Shanghai, China.

Abstract

Cohesin mediates chromatin loop formation across the genome by extruding chromatin between convergently oriented CTCF-binding elements. Recent studies indicate that cohesin-mediated loop extrusion in developing B cells presents immunoglobulin heavy chain (*Igh*) variable (V), diversity (D) and joining (J) gene segments to RAG endonuclease through a process referred to as RAG chromatin scanning. RAG initiates V(D)J recombinational joining of these gene segments to generate the large number of different *Igh* variable region exons that are required for immune responses to diverse pathogens. Antigen-activated mature B cells also use chromatin loop extrusion to mediate the synapsis, breakage and end-joining of switch regions flanking *Igh* constant region exons during class-switch recombination, which allows for the expression of different antibody constant region isotypes that optimize the functions of antigen-specific antibodies to eliminate pathogens. Here, we review recent advances in our understanding of chromatin loop extrusion during V(D)J recombination and class-switch recombination at the *Igh* locus.

Introduction

Mammalian genomes are folded into topologically associated domains characterized by increased contact frequency within the domains^{1,2}. These domains have been implicated in regulating various biological activities, including transcription³⁻⁹, replication^{10,11},

[†] yu.zhang@med.wmich.edu; alt@enders.tch.harvard.edu.

Author contributions

All authors contributed to writing the manuscript and/or designed and prepared the figures and legends.

Competing interests

The authors declare no competing interests.

Supplementary information

Supplementary information is available for this paper at <https://doi.org/10.1038/s415XX-XXX-XXXX-X>

recombination^{12,13} and DNA repair¹⁴⁻¹⁶, in part by promoting functional interactions between regulatory sequences and other sequences within the domains¹⁷. Many such domains are based on chromatin loops with well-defined boundaries anchored by CTCF-binding elements [G] (referred to in the remainder of the text as CTCF sites that are bound by the structural protein CTCF (CCCTC-binding factor) and by the cohesin ring protein complex [G]^{1,18} (Fig. 1). Cohesin-mediated chromatin loop extrusion modulates chromosome architecture by extruding chromatin between two CTCF sites of convergent orientation [G] to generate loop-shaped contact domains of up to millions of bases in size^{17,19-24}. Recent studies from our lab and others have advanced our mechanistic understanding of the genomic rearrangement processes in B cells that diversify antibody repertoires. These studies have shown that cohesin-mediated chromatin loop extrusion has fundamental roles in both V(D)J recombination [G]²⁵⁻²⁹ and class-switch recombination [G] (CSR) of the immunoglobulin heavy chain locus (*Igh*)^{30,31}.

Antibody subunits consist of pairs of identical immunoglobulin heavy chains and light chains. Highly diverse amino-terminal variable regions of the heavy and light chains provide antigen-binding specificity, and the carboxy-terminal heavy chain constant regions provide effector functions³². V(D)J recombination in developing B cells assembles germline gene segments into immensely diverse exons that encode the heavy and light chain variable regions³². In antigen-activated mature B cells, CSR replaces IgM-encoding constant region exons with a set of different downstream exons. CSR thus provides antigen-specific antibodies with a heavy chain constant region that is best suited for antigen elimination³³. The very different processes of V(D)J recombination and CSR both use chromatin loop extrusion to juxtapose cis-regulatory elements, substrate DNA sequences and initiating enzymes, as well as to promote the proper orientation of joined sequences^{26,30}. Here, we review recent advances in our understanding of the functions of chromatin loop extrusion in V(D)J recombination and CSR of the *Igh* locus.

Cohesin-mediated loop extrusion

CTCF sites are widely dispersed in the genome³⁴. However they are also highly enriched in certain loci, including the long locus that encodes IgH variable region gene segments^{35,36}. A substantial proportion of chromatin loops occur via cohesin binding to two widely separated CTCF-bound sites^{1,18}. CTCF binds these sites in an orientation-dependent manner^{37,38}. Thus, genomic CTCF sites can occur in the same orientation, divergent orientation or convergent orientation relative to each other¹⁸ (Fig. 1). Many major genomic contact loops have endpoints at convergently oriented CTCF sites bound by CTCF and, indirectly, by cohesin^{18,39,40}. Chromatin loops between convergent CTCF sites can be megabases long, and their orientation-specific bias cannot be readily explained by diffusion-based random collisions, which would be expected to promote the interaction of two CTCF sites independently of their chromosomal orientation^{21,22,24}. Thus, models of chromatin loop extrusion have posited that cohesin, upon loading onto chromatin primarily at enhancers and active promoters⁴¹⁻⁴³, actively drives the formation of contact loop domains by linearly extruding chromatin until extrusion is terminated in each direction upon reaching convergently oriented CTCF sites^{17,21-24} (Fig. 1).

Convergently oriented CTCF sites provide the strongest anchors for chromatin loops, largely owing to stabilization of cohesin through its interaction with the N-terminus of CTCF⁴⁴⁻⁴⁷. However, many studies indicate that these anchors are dynamic⁴⁸, in part owing to the continuous unloading and loading of CTCF at loop anchors^{49,50}. In addition, CTCF sites that are not in convergent orientation can function as weaker loop anchors⁵¹. Loop extrusion also can be impeded by other ‘obstacles’, for example transcription factors bound to enhancers and promoters^{17,51-53}. Therefore, loop boundaries formed by active enhancers and promoters may cooperate with CTCF sites to provide developmentally regulated sub-loops within larger loops based on CTCF sites^{25,26,30,54-56}. Deletion or mutation of convergent CTCF sites results in longer chromatin loop domains^{4,5,7,21}. Moreover, depletion of CTCF^{57,58} or cohesin⁵⁸⁻⁶¹, as well as inhibition of cohesin ATPase activity⁶², eliminates loop domains across the genome. Furthermore, depletion of WAPL (a protein that unloads cohesin) leads to increased retention of cohesin on chromatin^{63,64} and, thereby, extends chromatin loop length^{58,59,65}. This may reflect that the increased density of cohesin on chromatin provides more opportunities to extrude past dynamic CTCF-site anchors^{48,50}. Finally, elegant *in vitro* studies have shown that cohesin extrudes naked and nucleosome-bound DNA into loops⁶⁶⁻⁶⁸. Thus, the cohesin-mediated loop extrusion mechanism is now well accepted by the field^{48,51,52}.

V(D)J recombination

V(D)J recombination occurs during B cell development in the bone marrow. Progenitor B cells (pro-B cells) first assemble exons that encode *Igh* chain variable regions from V_H, D and J_H gene segments by V(D)J recombination. Subsequent IgH chain expression promotes development to the precursor B cell stage, during which immunoglobulin light chain (*Igl*) variable region exons are assembled from V_L and J_L segments. IgH and IgL chains associate to form the B cell receptor on immature B cells, which migrate to peripheral lymphoid organs to become mature B cells^{36,69}. Upon antigen activation, mature B cells can ultimately secrete their B cell receptor as antibodies. Studies of the role of chromatin loop extrusion in V(D)J recombination have mainly focused on the mouse 2.8 Mb *Igh* locus²⁵⁻²⁹ (Fig. 2a), and we refer to that locus here unless otherwise specified.

V(D)J recombination is initiated by RAG1–RAG2 endonuclease (collectively referred to here as RAG), which cleaves at the junctions between V, D and J coding segments and flanking recombination signal sequences (RSSs)⁷⁰. RSSs consist of a conserved heptamer (closely related to the sequence CACAGTG) and an AT-rich nonamer that are separated by a 12 base-pair spacer or a 23 base-pair spacer. These RSSs are referred to, respectively, as 12-RSSs and 23-RSSs (Fig. 2b). Such ‘bona fide’ RSSs flank gene segments in all antigen receptor loci that undergo V(D)J recombination, including immunoglobulin and T cell receptor loci. The first three nucleotides (CAC) of the heptamer define the RAG cleavage site and are crucial for RSS functionality⁷⁰. RAG also can target, at much lower levels, ‘cryptic’ RSSs that are not associated with V, D and J segments⁷¹. Such cryptic RSSs range from sequences similar to bona fide RSSs to sequences as simple as CAC^{12,71}. Robust RAG-mediated cleavage is restricted to paired gene segments that are flanked, respectively, by a bona fide 12-RSS or a 23-RSS⁷⁰. V_H segments are flanked by downstream 23-RSSs, D segments are flanked on both sides by 12-RSSs, and J_H segments are flanked by upstream

23-RSSs. This organization allows for V(D)J exon formation by the ordered joining of a D segment to a J_H segment and then a V_H segment to the DJ_H complex⁷² (Fig. 2c). Structural studies in the past decade provided a break-through in our understanding of V(D)J recombination. This work showed that RAG functions as a Y-shaped heterodimer in which active sites in the two RAG1 subunits bind a 12-RSS and a 23-RSS and align them for 12/23-restricted cleavage⁷³⁻⁷⁷ (Fig. 2d). RAG is not a classic ‘recombinase’ as the RSS and coding-segment ends cleaved by RAG are fused by classical non-homologous end-joining [G]^{78,79}.

Another advance in understanding V(D)J recombination was the discovery of the V(D)J recombination-centre [G]^{80,81}. In pro-B cells, an *Igh* V(D)J recombination-centre occurs in a 5-kb region of active chromatin spanning the J_H-proximal D segment DQ52, the 4 J_H segments and the intronic *Igh* enhancer iEμ⁸¹ (Fig. 2a). RAG binds the nascent V(D)J recombination-centre and upon acquisition of a J_H 23-RSS forms an activated J_H-based V(D)J recombination-centre for D-to-J_H joining^{25,53,71}. As DQ52 is located within the V(D)J recombination-centre, RAG can also initiate V(D)J recombination upon acquiring the DQ52 12-RSS²⁶. The intergenic control region 1 (IGCR1), which contains two CTCF sites, lies just upstream of the distal D segment DFL16.1^{82,83}, and a cluster of 10 CTCF sites lies just downstream (3′) of the *Igh* locus⁸⁴⁻⁸⁷. Interactions between the IGCR1 CTCF sites and the 3′ *Igh* CTCF sites were implicated in anchoring a chromatin loop that sequesters D segments and the recombination-centre away from V_H segments^{82,83} (Fig. 2e). The DJ_H intermediate then forms a new DJ_H-based V(D)J recombination-centre with its upstream D segment 12-RSS poised for V_H-to-DJ_H joining^{25,53}. Seminal 3D DNA fluorescence *in situ* hybridization (FISH) studies⁸⁸⁻⁹², augmented by chromatin conformation capture (3C)-based studies^{86,93-95}, discovered that the V_H locus undergoes physical contraction in primary pro-B cells. This process was implicated in bringing distant upstream V_H segments into close proximity to the DJ_H-based V(D)J recombination-centre to enable V_H-to-DJ_H joining^{36,96-99}. As discussed later in this Review, recent studies implicate a mechanistic role for chromatin loop extrusion in contraction of the V_H locus²⁷⁻²⁹.

Discovery of RAG chromatin scanning.

To test the potential of RAG-generated double-strand breaks to generate oncogenic translocations, a cassette containing 12/23-matched bona fide RSSs from D and J segments was inserted into the mouse *Myc* oncogene¹⁰⁰. This ‘*Myc*-DJ’ cassette was bred into an ATM-deficient background, which allows double-strand breaks to escape from normal C-NHEJ complexes and translocate^{101,102}. Strikingly, these mice developed B cell lymphomas with oncogenic chromosomal translocations that fused RAG-generated DNA breaks in the V(D)J recombination-centre with sequences far downstream of *Myc*¹⁰³. Notably, in mice heterozygous for the *Myc*-DJ cassette allele, translocations occurred exclusively on the cassette-containing allele, but did not involve the cassette¹⁰³. This finding suggested that RAG activity at bona fide D and J segment RSSs in *Myc* promoted ‘off-target’ activity far downstream in cis¹⁰³.

The mechanism of this long-range, off-target activity of RAG was elucidated in *v-Abl*-transformed pro-B cell lines derived from ATM-deficient mice carrying the *Myc*-DJ cassette

allele¹². Such *v-Ab1* cell lines can be viably arrested in G1 stage of the cell cycle, leading to the induction of RAG expression and V(D)J recombination at endogenous and chromosomally integrated cassette targets¹⁰⁴. These studies used high-throughput genome-wide translocation sequencing of V(D)J recombination outcomes (HTGTS-V(D)J-Seq [G]), which provides unprecedented sensitivity in elucidating RAG activity at both bona fide RSSs and cryptic RSSs^{12,53}. In addition to the great majority of joining products involving bona fide RSSs in the *Myc*-DJ cassette, a small subset of break ends in the cassette RSSs were joined to hundreds of cryptic RSSs within the 1.8 Mb downstream portion of the *Myc* loop domain¹² (Fig. 3a). Remarkably, these distant cryptic RSSs required as little as 3 base pairs (CAC) of the canonical RSS heptamer for paired cleavage and joining with a bona fide cassette RSS. In addition, cryptic RSSs were used predominantly when in convergent orientation with the cassette RSS to which they were joined¹². The dependence of this process on a convergent orientation suggested the involvement of active linear pairing, rather than diffusion-based random collisions^{12,17}. These findings were confirmed in primary pro-B cells¹².

Ectopic introduction of paired bona fide RSSs into 12 other chromatin loop domains across the genome that are known to be based on convergent CTCF sites showed that the orientation of each of the two initiating bona fide RSSs, respectively, programmed linear, directional chromatin exploration by RAG over long distances until the convergent CTCF sites-based loop boundary was reached¹² (Fig. 3b). In each of these chromatin loop domains, RAG predominantly targeted distant cryptic RSSs in convergent orientation with the initiating bona fide RSS¹². This process was originally referred to as RAG tracking, and cohesin was proposed as a driver¹² owing to similarities with proposed cohesin activities²². Contemporaneously with the RAG tracking study¹², two studies provided strong evidence in support of a proposed cohesin-driven chromatin loop extrusion model^{21,24}. Potential relationships between RAG tracking and cohesin-mediated loop extrusion were noted¹⁷. In this regard, RAG tracking and loop extrusion both are linear processes, both preferentially use RSSs or CTCF sites in convergent orientation, and both are restricted by the same loop anchors based on CTCF sites^{12,21,24,25,53}. Indeed, additional studies indicated that RAG tracking is more accurately described as RAG chromatin scanning, during which recombination-centre-bound RAG linearly scans chromatin presented by cohesin-mediated loop extrusion^{25,53}. Cohesin-depletion studies in G1-arrested *v-Ab1* cell lines provided direct evidence for the role of cohesin in this process²⁷.

RAG scanning mediates physiological D-to-J_H recombination.

Linear tracking had been long ago proposed to explain the highly preferential use of RSSs downstream, rather than upstream, of D segments to mediate D-to-J_H joining¹⁰⁵. However, extra-chromosomal plasmid studies dismissed tracking¹⁰⁵ or scanning¹⁰⁶ models for RAG activity in favour of diffusion-based models that proposed D segment downstream 12-RSSs had specialized properties for joining to J_H segment 23-RSSs¹⁰⁷. These models were revisited in a chromosomal setting in G1-arrested *v-Ab1* cell lines, which activate robust D-to-J_H joining; studies analyzed the effects of targeted mutagenesis of the endogenous D locus, including inversion of individual D segments and/or of upstream or downstream 12-RSSs²⁶. The findings implicated a linear RAG scanning mechanism in promoting deletional

D-to- J_H joining for all D segments except for DQ52 (see below), which is physically proximal to J_H segments in the V(D)J recombination-centre²⁶. (Fig. 4a). This process often may be initiated by cohesin loading in active chromatin in the region of the V(D)J recombination-centre (Fig. 4a, **parts ii-iv**). However, it also could be initiated by cohesin binding upstream of the recombination-centre with the same end result (Fig. 4a, **parts v and vi**). The V(D)J recombination-centre functions as a dynamic subdomain anchor that strongly impedes, but does not fully block, extrusion of downstream chromatin²⁵. Upstream chromatin extrusion is nearly fully blocked at the strong anchor mediated by the two IGCR1 CTCF sites^{25,26}. Overall, this process allows for upstream D-containing chromatin to be linearly presented to the open RAG1 active site opposite the bound J_H -RSS in the recombination-centre^{25,26}. During RAG scanning of upstream chromatin, convergent 12-RSSs downstream of D segments are captured, whereas 12-RSSs upstream of D segments in the same orientation as J_H segment 23-RSSs are almost invisible to RAG²⁶. These, and prior studies, showed that the preferential use of RSSs in convergent orientation is an intrinsic property of RAG scanning^{12,26}. To facilitate visualization of this process, we provide an animated model (Supplementary Video 1).

Given the very close proximity of DQ52 in the V(D)J recombination-centre to the J_H segments, both the upstream and downstream 12-RSSs of DQ52 should in theory access V(D)J recombination-centre-bound RAG by short-range diffusive motion, resulting in deletions and inversions during D-to- J_H joining^{12,26}. However, DQ52 joins to J_H segments predominantly by deletion. To resolve this potential paradox, DQ52 and its RSSs were inverted in the V(D)J recombination-centre location, leading to predominantly inversional DQ52-to- J_H joining mediated by the 12-RSS that is normally downstream of DQ52 but now placed in a divergent orientation upstream of DQ52. Thus, DQ52 seems to have evolved a dominant downstream 12-RSS¹⁰⁷. This dominant downstream 12-RSS in its normal location in the V(D)J recombination-centre promotes deletional joining to J_H and obviates diffusion-mediated inversional joining by the weaker upstream 12-RSS²⁶. When DQ52 was inserted, in its normal orientation, far upstream in place of DFL16.1, it also was highly used for deletional joins mediated by its robust downstream 12-RSS. However, when DQ52 was inverted in this far upstream location, the weaker 12-RSS normally upstream of DQ52, now in a downstream orientation convergent to J_H , became predominantly used to mediate deletional J_H joining²⁶ (Fig. 4b). This set of experiments provided clear evidence that linear RAG scanning enforces the deletional joining of D segments that lie distal to the V(D)J recombination-centre²⁶. Finally, when DQ52 was inverted in the DFL16.1 position, its dominant 12-RSS, now in the upstream position, mediated low-level inversional joining to J_H (Fig. 4b). A model to explain this latter finding proposed that the strong RSS in upstream position gains low-level access to V(D)J recombination-centre-bound RAG via short-range diffusional motion when brought into proximity by loop extrusion²⁶ (Fig. 4b). Related diffusional mechanisms might contribute more prominently to programmed inversional V(D)J recombination at other antigen receptor loci, including long-range inversional joining within the *Igk* light chain locus (Box 1).

V_H accessibility during RAG chromatin scanning.

All V_H segments and their associated 23-RSSs lie in convergent orientation with the upstream 12-RSSs of D segments of the DJ_H-based V(D)J recombination-centre³⁶. In this regard, early findings that the D-proximal V_H segments are the most frequently rearranged suggested a role for linear scanning¹⁰⁶. However, that study pointed out the complicating factor that the D-proximal V_{H5-1} barely rearranges, despite its consensus bona fide 23-RSS¹⁰⁶. Remarkably, all of the D-proximal V_H segments, except for V_{H5-1}, have CTCF sites directly downstream of their 23-RSSs^{25,36,85,108,109}. To test the potential roles of these CTCF sites in promoting rearrangement, the CTCF site of the most highly rearranging V_{H5-2} (also known as V_{H81X}), which lies just upstream of V_{H5-1}, was mutationally inactivated, which nearly abrogated use of V_{H5-2} in primary pro-B cells, despite its bona fide 23-RSS²⁵. For further analysis, G1-arrested *v-Ab1* cells were used, which do not undergo V_H locus-contraction or distal V_H-to-DJ_H rearrangement²⁵. Indeed, in *v-Ab1* cells, linear scanning upstream of the DJ_H-based V(D)J recombination-centre is largely blocked at the IGCR1 anchor^{12,25}. However, mutational inactivation of IGCR1 CTCF sites in *v-Ab1* cells extended RAG scanning through the 100kb intervening region containing IGCR1 to the most proximal V_H segments^{12,25}. Moreover, IGCR1 inactivation greatly increased interactions between V_{H5-2} and the DJ_H-based V(D)J recombination-centre and, correspondingly, increased its rearrangement frequency about 50-fold^{12,25,82,83} (Fig. 4c). Remarkably, inactivation of the V_{H5-2}-associated CTCF site in the context of IGCR1 inactivation still nearly abrogated interaction of V_{H5-2} with the V(D)J recombination-centre and its high-level rearrangement. Moreover, inactivation of the V_{H5-2} CTCF site promoted robust scanning upstream to the next V_H segment V_{H2-2}, which became highly used²⁵. These results solved the mystery of low-level V_{H5-1} rearrangement, owing to its lack of a downstream CTCF site. Conversion of a non-functional sequence just downstream of V_{H5-1} into a functional CTCF site promoted robust interaction of V_{H5-1} with the V(D)J recombination-centre and rendered it, by far, the most frequently rearranged V_H²⁵.

These studies showed that the convergent RSSs of proximal V_H segments alone do not promote robust rearrangement during linear RAG scanning and that proximal V_H CTCF sites are required to enhance chromatin accessibility²⁵. This function, which is not absolutely dependent on orientation of the CTCF site, is based on the ability of V_H-associated CTCF sites, but not RSSs, to impede loop extrusion and, thereby, prolong interaction with the V(D)J recombination-centre²⁵ (Fig. 4c). Although proximal V_H-associated CTCF sites do not create absolute boundaries for loop extrusion and RAG scanning, the first few proximal V_H segments that are encountered dominate recombination-centre interactions and rearrangements in *v-Ab1* cells, albeit at progressively decreasing levels as expected for a linear process (Fig. 4c).

Loop extrusion promotes V_H locus contraction and scanning.

Many of the 109 V_H segments in the mouse genome lie in a 2.4 Mb region upstream of the proximal V_H segments that harbours numerous CTCF-bound sites. Unlike the proximal V_H-associated CTCF sites, upstream CTCF sites are not directly adjacent to V_H segments^{25,36,85,108,109}, which suggests that they might have different or additional roles. The CTCF sites of the V_H locus are in convergent orientation with the ten 3' CTCF sites

downstream of the *Igh* locus³⁶ and have substantial interactions with them^{86,93}. In this regard, loop extrusion has been considered as a mechanism for locus contraction^{27-29,110}. However, CTCF-bound sites across the V_H locus would be impediments to linear loop extrusion²⁵, unless their inhibitory activity as observed in *v-Abl* cells is somehow reduced in primary pro-B cells²⁷. Notably, CTCF depletion in non-lymphoid cells suppresses most CTCF site-based chromatin interactions across the genome^{57,58}. To test the potential negative effects of CTCF-bound sites on locus contraction and long-range RAG scanning, CTCF was depleted in G1-arrested *v-Abl* cells²⁷, which reduced interactions of the recombination-centre with IGCR1 CTCF sites and the CTCF sites of the most proximal V_H segments. By contrast, CTCF depletion promoted robust recombination-centre interactions across the distal V_H locus, with hallmarks of locus contraction essentially identical to those in locus-contracted primary pro-B cells²⁷. Correspondingly, CTCF depletion activated robust distal V_H-to-DJ_H joining in *v-Abl* cell lines. In these studies, free CTCF was eliminated but chromatin-bound CTCF remained associated at lower levels with certain CTCF sites²⁷. Thus, it is proposed that bound CTCF was sufficiently depleted to allow for loop extrusion-mediated RAG scanning to frequently pass IGCR1 and V_H locus CTCF sites, but that residual CTCF at some sites promoted recombination-centre interactions and use during scanning²⁷. These studies provided proof-of-principle in cell lines that downmodulation of CTCF site impediments activates locus contraction and long-range RAG scanning. However, addressing the mechanism that operates in primary pro-B cells required different approaches.

Cryptic RSS use supports long-range V_H locus scanning.

A diffusion-based model of access to distal V_H segments, in its simplest form, predicts little impact of V_H RSS orientation on access to the DJ_H-V(D)J recombination-centre. By contrast, a linear scanning model predicts that inverting the normally convergent V_H RSS to the same orientation as the RSS of the DJ_H-V(D)J recombination-centre would markedly decrease its rearrangement. To distinguish between these two models, one study inverted an 890 kb portion of the distal V_H locus²⁸, and a second study inverted a 2.4 Mb portion of the V_H locus, leaving D-proximal V_H5-2 in its normal position and orientation²⁹. V_H rearrangements were essentially abrogated in both inverted regions, whereas V_H segments left in their normal orientation were still rearranged^{28,29} (Fig. 5a).

To assess effects of the 2.4 Mb inversion on *Igh* chromatin interactions, a LAM-HTGTS-3C-Seq [G] approach was used²⁵. Such chromatin interaction assays must be carried out in RAG-deficient *v-Abl* or primary pro-B cells to obviate confounding changes in genome organization associated with V(D)J recombination^{25-27,29}. In primary pro-B cells, the recombination-centre interacts robustly with about 15 highly focused regions²⁹, many of which have been speculated to be involved in locus contraction⁹³. Among the most robust are the PAX5-activated intergenic repeat (PAIR) elements^{93,97,111,112} in the distal V_H locus. Remarkably, all major recombination-centre-V_H locus interactions were maintained within the inverted V_H locus as mirror images²⁹. Transcription profiles were precisely maintained across the inverted locus, albeit in the opposite direction relative to the recombination-centre. Nearly all CTCF sites spread over a 1 Mb distal region of the locus maintained similar levels of interactions with the 3' CTCF sites downstream of the *Igh* locus when

they were inverted and moved into a proximal position, but the 37 functional V_H segments inverted in this region still did not rearrange²⁹.

HTGTS-V(D)J-Seq analyses revealed that in normal V_H loci, RAG uses, in addition to convergently oriented bona fide V_H RSSs, hundreds of convergent cryptic RSSs embedded across the V_H locus²⁹ (Fig. 5b). Use of these normally convergent cryptic RSSs was abrogated in the inverted V_H locus, which is fully consistent with a linear scanning mechanism for RAG. Strikingly, however, cryptic V_H-locus RSSs normally in the same orientation as the RSS of the DJ_H-V(D)J recombination-centre became robustly used when placed in a convergent orientation upon locus inversion²⁹ (Fig. 5b). These studies show that RAG scans the entire inverted V_H locus from its DJ_H-recombination centre location, although not necessarily from the same starting point in the V_H locus (as described later). Correspondingly, the inability of inverted bona fide V_H RSSs to be rearranged during RAG linear scanning of the V_H locus, similarly to the RSSs upstream of D segments, predominantly reflects their inability to be properly paired^{28,29} (Fig. 5c)

WAPL downregulation promotes long-range scanning of the V_H locus.

Inversion of the 2.4 Mb V_H locus in primary pro-B cells extended the scanning activity of V(D)J recombination-centre-bound RAG to cryptic RSSs beyond the V_H locus by extending loop extrusion through multiple convergently oriented CTCF sites to the telomere (Fig. 5b, c). This finding indicated that CTCF site-mediated impediments to loop extrusion are broadly deregulated in primary pro-B cells, both in the *Igh* locus and beyond²⁹. An interesting unsolved question is why RAG scanning proceeds beyond the V_H locus in pro-B cells with an inverted *Igh* locus but not in those with normally oriented V_H segments. One possibility could be decreased impedance of loop extrusion by normally proximal CTCF sites when they are inverted in a distal position²⁹.

Strikingly, 3C-based Hi-C studies of chromatin interactions indicated that chromatin loops are extended across the genome in primary pro-B cells²⁸. To identify factors associated with the cohesin complex that might be deregulated to allow for such extended chromatin looping and scanning in primary pro-B cells, both of the V_H locus inversion studies looked for factors that are differentially expressed in primary pro-B cells compared with earlier or later developmental stages and/or *v-Ab1* cell lines^{28,29}. Both studies identified the WAPL cohesin-unloading protein as one such factor^{28,29}. As mentioned above, WAPL depletion in non-lymphoid cells increases the size of CTCF-anchored loops genome wide^{58,59,65}. Thus, WAPL downregulation in pro-B cells was a strong candidate for promoting enhanced loop extrusion past CTCF site-based V_H locus impediments.

The transcription factor PAX5 has long been known to be required for locus contraction and recombination of distal V_H segments^{89,113}, with one postulated mechanism involving transcription of PAIR elements in the distal V_H locus^{97,111,112}. However, an elegant recent study discovered that PAX5 achieves this function by mediating developmental reduction of *Wapl* expression in pro-B cells²⁸. PAX5 suppresses *Wapl* transcription by engaging a PAX5-binding element in the *Wapl* promoter and then recruiting the polycomb repressive complex 2 (PRC2) to induce repressive H3K27me3 histone methylation²⁸. Remarkably, deletion of this PAX5-binding element resulted in loss of V_H locus contraction and distal

V_H rearrangements in pro-B cells²⁸. These studies further revealed that an approximately four-fold reduction in *Wapl* expression is sufficient for locus contraction and distal V_H rearrangement²⁸. Although this reduction in *Wapl* expression also altered genome-wide chromatin architecture, it did not impact gene expression required for pro-B cell survival²⁸. A contemporaneous study showed that depleting WAPL in G1-arrested *v-Ab1* cells activated V_H locus contraction and V(D)J recombination across the entire upstream V_H locus²⁹. Moreover, WAPL-depleted *v-Ab1* lines with the 2.4 Mb V_H locus inversion had the same phenotype as primary pro-B cells with this inversion, with respect to both effects on the use of bona fide and cryptic RSSs and the activation of RAG scanning upstream of *Igh* to the telomere²⁹. In support of increased cohesin processivity in WAPL-depleted *v-Ab1* lines, cohesin was redistributed to distal V_H regions and to the 3' *Igh* CTCF sites, similar to the distribution observed in primary pro-B cells²⁹. Overall, this work showed that WAPL downregulation neutralizes the impediments to V_H locus contraction and distal V_H rearrangement that would otherwise be mediated by CTCF sites in pro-B cells^{28,29}.

Substrate accessibility during V(D)J recombination.

V(D)J recombination is regulated epigenetically by modulating the chromatin accessibility of substrate V, D and J segments to RAG activity³². Factors implicated in determining accessibility include sense and antisense transcription and active chromatin^{32,96,114-117}. New insights into regulating accessibility have recently come from studies of *v-Ab1* cell lines in which downstream-oriented RSSs in the V(D)J recombination-centre programme robust RAG scanning across the downstream C_H-containing domain to the 3' CTCF sites²⁶ (Fig. 6a, **parts i-v**). This downstream *Igh* domain lacks dominant bona fide RSSs or CTCF sites that impede scanning, which allows for accessibility mechanisms to be more readily revealed.

In these *v-Ab1* cells, a 7kb repetitive switch region [**G**] (S region) that is constitutively transcribed functions as a dynamic loop extrusion anchor and, thereby, targets downstream RAG scanning to cryptic RSSs located all across it²⁶. Indeed, deletion of the S region promoter abrogated transcription, V(D)J recombination-centre interactions and the ability to target RAG scanning, all in association with allowing loop extrusion to proceed through this S region unimpeded²⁶. This work indicated that transcription, similarly to CTCF-bound sites, can target a sequence for accessibility during RAG scanning by increasing its interaction with the recombination centre²⁶ (Fig. 6a, **part iv**). A related study revealed that binding of catalytically 'dead' Cas9 (without endonuclease activity but which retains specific DNA-binding activity) to 16 repeated target sites in a different, untranscribed S region also impeded RAG scanning and focused RAG activity to convergent cryptic RSSs within it²⁶ (Fig. 6a, **part iii**). This latter study suggested that binding of 'dead' Cas9 may sterically hinder RAG scanning. However, a caveat was that binding of 'dead' Cas9 promoted accumulation of the cohesin loader NIPBL and of cohesin across the region, which raises the possibility of an indirect inhibition mechanism²⁶.

Analyses of various parameters for individual V_H segments in primary pro-B cells and in WAPL-depleted *v-Ab1* lines implicated CTCF site activity and/or transcription in enhancing the accessibility of their RSSs^{25,27,29}. Proximal V_H segments lack detectable transcription

and their use correlates with impediments to further scanning mediated by CTCF sites²⁵. By contrast, all highly rearranged distal V_H segments are transcribed; although not all transcribed segments are highly rearranged^{27,29}. Most of the highly rearranging, transcribed distal V_H segments also have CTCF-bound sites within 10 kb that could conceivably function with transcription to enhance interaction of the region containing them with the V(D)J recombination-centre during RAG scanning²⁹. Finally, some frequently rearranged V_H segments in the middle of the V_H locus lack closely associated CTCF-bound sites and are not transcribed, which suggests that other accessibility factors remain to be elucidated^{27,29}.

Summary of loop extrusion-based models for V(D)J recombination at the Igh locus.

Igh locus V(D)J recombination is predominantly initiated from the V(D)J recombination-centre, which harbours the vast majority of bound RAG^{80,81}. Current findings indicate that the V(D)J recombination-centre also functions as a major downstream anchor for loop extrusion-mediated RAG scanning of upstream chromatin^{25-27,29}. The 3' CTCF sites downstream of the *Igh* locus have also been proposed to have roles in anchoring loop extrusion during long-range *Igh* V(D)J recombination^{25,28,110}. Similarly to other CTCF sites genome wide, the 3' *Igh* CTCF sites impede RAG scanning²⁶. Thus, the 3' CTCF sites might reinforce the loop anchor provided by the V(D)J recombination-centre upon their extrusion-mediated juxtaposition. Surprisingly, however, recent studies have shown that complete deletion of the 3' *Igh* CTCF sites has little impact on *Igh* V(D)J recombination²⁹. But, as described for CSR below, other CTCF sites further downstream may be extruded to the recombination centre and compensate for the putative functions of the 3' CTCF sites in their absence^{29,30}.

The initial D-to-J_H V(D)J recombination step incorporates both short-range diffusion and long-range RAG scanning. Owing to its location in the V(D)J recombination-centre, the frequently used DQ52 accesses RAG mainly by short-range diffusional motion²⁶. Indeed, loop extrusion is thought to counteract even more dominant use of DQ52 by quickly isolating it from recombination centre-bound RAG^{26,118}. All D segments upstream of the V(D)J recombination-centre are accessed primarily by linear RAG scanning²⁶ (Fig. 4a). The very frequent use of distal DFL16.1 may reflect prolonged interaction with the V(D)J recombination-centre owing to scanning being impeded by the IGCR1 CTCF sites^{26,119}. Robust transcription of the IGCR1–DFL16.1 region may also contribute to its high-level targeting during RAG scanning²⁶. Lower-level targeting of intervening D segments also may be mediated by their antisense transcription^{26,117,120}.

IGCR1 prevents direct joining of V_H segments to D segments^{82,83}. In pro-B cells, *Wapl* downregulation suppresses IGCR1-based and other V_H locus impediments to RAG scanning sufficiently to promote V_H locus contraction and the use of V_H segments across the locus²⁹. In theory, D-to-J_H joining might activate *Wapl* downregulation to enable locus contraction. However, locus contraction also occurs in RAG-deficient pro-B cells in the absence of V(D)J recombination^{88,89,93}. Thus, PAX5-mediated downregulation of *Wapl* expression may be an early event associated with differentiation to the pro-B cell stage. If so, D-to-J_H rearrangements may occur first owing to their proximal position to the V(D)J

recombination-centre during scanning. Understanding how the persisting activity of CTCF sites following a four-fold reduction in WAPL levels, together with transcription and other factors, contribute to the rearrangement levels of each V_H segment across the loop extrusion path remains an interesting challenge.

How RAG scanning promotes diverse distal V_H use in the face of downstream scanning impediments and proximal V_H rearrangements after *Wapl* downregulation is another challenging question. One model suggests that pro-B cells often initiate loop extrusion of upstream chromatin past nascent V(D)J recombination-centres that progresses to various distances across the V_H locus in individual cells²⁹ (Fig. 6b). Subsequent RAG binding to extruded nascent V(D)J recombination-centres could then generate active V(D)J recombination-centres at various points across the V_H locus²⁹ (Fig. 6c). Extrusion of downstream chromatin from cohesin bound to distal V_H domains with high transcriptional activity could also mediate this process. Such a mechanism could minimize the potential competitive advantages of D-proximal V_H segments during scanning to ensure the generation of diverse antibody repertoires²⁹.

Another recent report proposes a model in which loop extrusion and diffusional access cooperate to promote distal V_H use²⁸. This model suggests that 3' *Igh* CTCF sites and convergent V_H locus CTCF sites anchor 'stable' chromatin loops that allow for V_H segments within the loop to access the V(D)J recombination-centre by diffusion²⁸. As currently proposed, this diffusion-based model does not readily explain the long-range orientation-specific use of cryptic RSSs across normal and inverted V_H loci. However, this report proposes a second model in which orientation specificity is mediated by the alignment of convergent V_H region RSSs and V(D)J recombination-centre RSSs for deletional joining via linear loop extrusion²⁸. This second model is very similar to the linear RAG scanning model with one exception^{27,29} in that it proposes no role for the well-documented ability of the V(D)J recombination-centre to function as an extrusion anchor that increases the frequency of relevant interactions^{25-27,29}.

Class-switch recombination

Exons encoding the immunoglobulin heavy-chain constant (C_H) regions lie within a downstream 250kb *Igh* subdomain that lacks CTCF sites. Transcription from an assembled V(D)J exon runs through C_μ exons encoding the C-terminal C_H region that specifies IgM. Upon activation, mature B cells undergo CSR to replace the C_μ exons with one of 6 sets of C_H exons in the 100–200kb downstream subdomain³³ (Fig. 7a). Each set of these C_H exons ($C\gamma 3$, $C\gamma 1$, $C\gamma 2a$, $C\gamma 2b$, $C\epsilon$ and $C\alpha$) specifies an antibody class with different effector properties and functions¹²¹. Long, repetitive S regions (up to 12kb) precede C_μ and each downstream C_H ¹²¹. Activation-induced cytidine deaminase (AID)¹²² initiates CSR by generating deamination lesions at short target motifs within donor S_μ and a downstream acceptor S region^{33,123}. These lesions are converted into double-strand breaks by co-opted general DNA repair pathways^{33,123,124}. Deletional end-joining of the upstream end of an S_μ double-strand break to the downstream end of an acceptor S region double-strand break completes productive CSR in mice and humans¹³ (Fig. 7a).

Enhancers at either end of the C_H-containing *Igh* subdomain have important roles in CSR. Deletion of iE μ variably reduces CSR¹²⁵⁻¹²⁸. The 27kb 3' *IghRR* super-enhancer at the downstream end of this subdomain contains closely associated enhancers that are essential for transcription from S region promoters (I-promoters) to induce transcriptionally mediated CSR¹²⁹⁻¹³². Early 3C studies detailed the interaction patterns of the 3' *IghRR* and iE μ with different C_H regions in resting and CSR-stimulated wild-type B cells that corresponded to I-promoter transcription and associated patterns of CSR¹³². These seminal studies suggested that interactions of 3' *IghRR* with upstream I-promoters form a 'synaptosome' that determines the potential for germline transcription and CSR to associated S regions¹³². The mechanism by which synaptosome structures are formed between widely separated *Igh* sequences remained unclear. However, other early studies provided a mechanistic hint with the finding that I-promoters located across a 100kb upstream region undergo linear competition for 3' *IghRR*-mediated activation to promote CSR¹³³.

Because S regions are up to 12kb long and repetitive, prior CSR assays yielded few CSR junctions, all from S region borders, and gave limited mechanistic insights. Based on studies in transformed cell lines, DNA breaks were proposed to join at similar levels by inversional and deletional joining during CSR, with cellular selection required to sort out productive deletional rearrangements¹³⁴. However, a recently developed high-throughput, highly sensitive LAM-HTGTS-Seq CSR assay has identified tens of thousands of CSR junctions across the entire length of acceptor S regions in CSR-activated normal B cells¹³. This assay revealed that AID-initiated double-strand breaks during CSR arise from most of the hundreds of deamination motifs across S regions and confirmed that donor and acceptor S region breaks can be generated independently of S region synapsis¹³. Moreover, this assay revealed that the great majority of CSR joining events between donor S μ and acceptor S regions occur in deletional orientation by an unknown mechanism involving *Igh* organizational features in cis¹³ (Fig. 7a). This finding was striking as, other than V(D)J recombination-associated double-strand breaks, most breaks ends genome wide join to the ends of other separate double-strand breaks without orientation bias^{13,135-137}. The orientation specificity of CSR was puzzling as there was no known factor, similar to RAG, that could enforce the orientation-specific AID-initiated joining of double-strand breaks. These findings pointed to an active synapsis mechanism during CSR³⁰.

Chromatin loop extrusion-mediated CSR.

Indeed, recent studies have shown in three ways that cohesin-mediated loop extrusion is the fundamental mechanism of CSR³⁰ (Fig. 7b; Supplementary Video 2).

First, in resting B cells, the iE μ -S μ region and the 3' *IghRR* load cohesin and also function as dynamic loop extrusion anchors (Fig. 7b, **part i**). Cohesin-mediated extrusion of chromatin between these two dynamic loop anchors leads to the formation of basal, dynamic CSR loops and a class-switch recombination-centre [**G**] (CSR-centre) that is dynamic and likely to be deformed and reformed in resting B cells³⁰.

Second, in activated B cells, the 3' *IghRR*, donor S μ and acceptor S region are actively aligned in the CSR-centre by an activation-induced secondary loop extrusion process that

is not dependent on expression of AID³⁰. Although downstream S regions in the basal CSR loop are constantly extruded through the CSR-centre, they do not impede further extrusion as they are not transcribed and are inert in this regard. However, priming of a particular I region promoter through B cell activation and/or cytokine stimulation leads to transcriptional activation when it is brought proximal to the 3' *IghRR* in the CSR-centre (Fig. 7b, **part ii**). Induced I-region transcription leads to binding of the cohesin loader NIPBL and of cohesin at the activated I region promoter and the extrusion of a new sub-loop that aligns the activated downstream S region and S μ in the CSR-centre³⁰ (Fig. 7b, **part iii**). B cell activation also induces AID expression, which targets actively aligned S region double-strand breaks¹³⁸.

Third, physical synapsis of individual double-strand break ends in each synapsed S region for deletional CSR is mediated post-cleavage by a loop extrusion-related mechanism³⁰. Thereby, double-strand breaks on S μ and the target S region can occur at different times and locations along the S region, as one or both ends of a given S region double-strand break is extruded into an associated cohesin ring, thereby stalling extrusion (Fig. 7b, **part iv**). The ends of a double-strand break in the second synapsed S region would then be extruded into the same cohesin ring(s), which aligns donor and acceptor break ends for productive, deletional joining³⁰ (Fig. 7b, **parts v and vi**). Notably, this loop extrusion-mediated alignment process can be impaired by the insertion of CTCF sites within the extrusion path, leading to incomplete alignment and increased inversional joining. Such inversional CSR probably occurs because misaligned S regions are brought into close enough proximity for double-strand break ends in the donor and acceptor S regions to access each other by short-range diffusional motion³⁰. Structural variations in chicken¹³⁹ and duck¹⁴⁰ C_H loci may similarly promote inversional joining between oppositely oriented donor and acceptor S regions, with cellular selection for productive inversional events during CSR.

The above findings in support of a loop extrusion-mediated model of CSR indicate an unappreciated role for *Igh* enhancers and associated sequences in CSR. Namely, the enhancers function as cohesin loading sites and dynamic impediments to loop extrusion that are crucial for S region synapsis³⁰. Similarly to V(D)J recombination²⁵, impeding extrusion past a CSR-centre promotes the accessibility of impeded acceptor S regions for AID-mediated breakage and subsequent joining to S μ ³⁰. Notably, insertion of CTCF sites in the CSR scanning path leads to misalignment of adjacent downstream non-S region sequences with S μ , causing them to become surrogate S regions that undergo AID-initiated double-strand breaks and joining to S μ ³⁰. Finally, loop extrusion-mediated CSR provided a mechanism for the enigmatic "sequential" CSR (from S μ to S γ 1 and then S μ /S γ 1 to S ϵ)^{141,142} and "downstream" CSR (between S γ 1 and S ϵ)¹⁴³ events that contribute to IgE antibody generation³⁰ (ref 30; supplemental discussion).

3' *Igh* CTCF sites prevent ectopic CSR-centre formation.

The 3' *Igh* CTCF sites focus chromatin loop extrusion-mediated activities within the upstream C_H-containing domain and prevent 3' *IghRR*-mediated transcription and CSR downstream of the *Igh* locus^{31,144}. Thus, deleting all ten 3' *Igh* CTCF sites in mice significantly decreases the transcription, synapsis and switching of upstream S regions to

varying degrees³¹. Moreover, deletion of the 3' CTCF sites leads to active transcription of non-*Igh* downstream sequences, which allows for these sequences to be synapsed with S μ to become ectopic S regions³¹.

Potential related roles of loop extrusion in double-strand break repair.

A recent study revealed that double-strand breaks may stall loop extrusion on one side of each break end, allowing extrusion to continue on the other sides¹⁵. This mechanism may enable the DNA-damage response protein ATM to scan the chromatin that is extruded past cohesin-bound double-strand break ends and phosphorylate other damage response proteins until arrested by loop anchors to form characteristic foci¹⁵. This mechanism is potentially related to the proposed mechanism of loop extrusion in tethering double-strand break ends for proper joining during CSR³⁰ and provides a mechanism for early chromatin compaction models for the tethering of S region breaks for CSR¹⁴⁵. This new study, together with related findings^{146,147}, implicates an important role for cohesin-mediated loop extrusion in the maintenance of genome stability through double-strand break repair¹⁴⁸.

Concluding remarks

Although tremendous progress has been made in understanding the roles of chromatin loop extrusion in RAG scanning and CSR, further studies are required of these dynamic processes, which are likely far more complex than outlined in current models. Similarly, the detailed mechanisms by which various factors promote the accessibility and pairing of target sequences within V(D)J recombination-centres and CSR-centres is another important area for further investigation. A long-standing question has been whether locus contraction involves an active mechanism in G1-arrested pro-B cells or whether the process requires cell-cycle progression³². The implicated role of cohesin-mediated loop extrusion in locus contraction may provide an insight. Specifically, cohesin-mediated chromatin loops are disassembled during mitosis and reassembled in G1⁴⁸. As V(D)J recombination is shut down upon G1 exit¹⁴⁹, the prime opportunity for loop extrusion-mediated locus contraction to intersect with V(D)J recombination would seem to be in G1. Extension of current population-based studies to single-cell resolution may be required to fully elucidate these mechanisms.

Supplementary Material

Refer to Web version on PubMed Central for supplementary material.

Acknowledgements

This work was supported by US National Institutes of Health grants (R01AI020047 and R01AI077595 to F.W.A.; R01AI155775 to Y.Z.). H.-Q.D. was a fellow of the Cancer Research Institute (CRI) of New York. H.H is a fellow of CRI. F.W.A. is an investigator of the Howard Hughes Medical Institute.

Glossary

CTCF-binding elements

(CTCF sites). DNA sequence motifs recognized by the structural protein CTCF (CCCTC-binding factor) that mostly are characterized by a highly conserved 20 base pair core consensus motif but a subset of which are also flanked by upstream and/or downstream regulatory motifs.

Cohesin ring protein complex

A highly conserved ring-shaped multi-protein complex composed of three core subunits, SMC1, SMC3 and RAD21, that associate with SA1 or SA2 in somatic cells. The cohesin complex has ATPase activity and has essential functions in chromosome segregation and chromatin loop formation, as well as in various fundamental processes including transcription and DNA repair.

Convergent orientation

Referring to two DNA sequence motifs of opposite orientation that point towards each other in cis.

V(D)J recombination

A programmed somatic recombination process initiated by RAG1–RAG2 endonuclease in early developing lymphocytes that assembles V, D and J gene segments into exons that encode the variable regions of antibody and T cell receptor chains.

Class-switch recombination

(CSR). A programmed somatic recombination process initiated by activation-induced cytidine deaminase in antigen-activated mature B cells that replaces the upstream IgM-encoding C μ exon with a different downstream constant region exon to change the class of antibody expressed. This allows for the antigen-specific effector functions of an antibody with a given variable region specificity to be optimized.

Classical non-homologous end-joining

A major cellular repair pathway for DNA double-strand breaks that joins DNA ends without requiring a homologous template. This pathway is commonly referred to as ‘classical’ to distinguish it from less robust alternative end-joining pathways that become more obvious in the absence of the classical pathway.

V(D)J recombination-centre

In the *Igh* locus, this is the site where RAG1–RAG2 endonuclease binds active chromatin harboring a strong enhancer to generate a hub for the capture of substrate V, D and J segments to allow for their cleavage and joining to create V(D)J variable region exons. Similar recombination-centres occur in the other antigen receptor loci that undergo V(D)J recombination.

HTGTS-V(D)J-Seq

This assay maps RAG-initiated V(D)J recombination events across the genome and is adapted from the linear amplification-mediated high-throughput genome-wide translocation sequencing method (LAM-HTGTS). HTGTS-V(D)J-Seq has a unique ability to detect thousands of low-level independent cryptic joining events within a large population of cells, that when viewed together provide ‘tracks’ of RAG activity within a domain. These

tracks clearly show the chromatin regions that recombination-centre-bound RAG explores, the directionality of the exploration process and the sequences RAG does or does not ‘see’ during exploration.

LAM-HTGTS-3C-Seq

A high-resolution chromatin conformation capture (3C)-based genomic interaction assay that uses linear amplification-mediated high-throughput genome-wide translocation sequencing (LAM-HTGTS) for its downstream steps. This method detects sequences within chromatin loop domains that interact with a sequence of interest at high resolution.

Switch region

(S region). A 1–12 kb repetitive DNA sequence that precedes each set of *Igh* constant region exons. S regions undergo DNA double-strand breaks mediated by activation-induced cytidine deaminase that are then joined to effect IgH class-switch recombination.

Phase separation

A process that forms condensates of loci with similar chromatin states through homotypic attraction of bridging proteins.

Class-switch recombination-centre

(CSR-centre). The CSR-centre is an *Igh* locus site at which activated B cells juxtapose distant *cis*-regulatory elements with donor and acceptor DNA switch regions, which are then cleaved and joined to carry out the process of antibody isotype switching.

References

1. Dixon JR et al. Topological domains in mammalian genomes identified by analysis of chromatin interactions. *Nature* 485, 376–380 (2012). [PubMed: 22495300]
2. Nora EP et al. Spatial partitioning of the regulatory landscape of the X-inactivation centre. *Nature* 485, 381–385 (2012). [PubMed: 22495304]
3. Downen JM et al. Control of cell identity genes occurs in insulated neighborhoods in mammalian chromosomes. *Cell* 159, 374–387 (2014). [PubMed: 25303531]
4. Lupianez DG et al. Disruptions of topological chromatin domains cause pathogenic rewiring of gene-enhancer interactions. *Cell* 161, 1012–1025 (2015). [PubMed: 25959774]
5. Narendra V et al. CTCF establishes discrete functional chromatin domains at the Hox clusters during differentiation. *Science* 347, 1017–1021 (2015). [PubMed: 25722416]
6. Hnisz D, Day DS & Young RA Insulated Neighborhoods: Structural and Functional Units of Mammalian Gene Control. *Cell* 167, 1188–1200 (2016). [PubMed: 27863240]
7. Merkenschlager M & Nora EP CTCF and Cohesin in Genome Folding and Transcriptional Gene Regulation. *Annu. Rev. Genomics Hum. Genet* 17, 17–43 (2016). [PubMed: 27089971]
8. Stadhouders R, Filion GJ & Graf T Transcription factors and 3D genome conformation in cell-fate decisions. *Nature* 569, 345–354 (2019). [PubMed: 31092938]
9. Guo Y et al. CRISPR Inversion of CTCF Sites Alters Genome Topology and Enhancer/Promoter Function. *Cell* 162, 900–910 (2015). [PubMed: 26276636]
10. Pope BD et al. Topologically associating domains are stable units of replication-timing regulation. *Nature* 515, 402–405 (2014). [PubMed: 25409831]
11. Moindrot B et al. 3D chromatin conformation correlates with replication timing and is conserved in resting cells. *Nucleic Acids Res.* 40, 9470–948 (2012). [PubMed: 22879376]
12. Hu J et al. Chromosomal Loop Domains Direct the Recombination of Antigen Receptor Genes. *Cell* 163, 947–959 (2015). [PubMed: 26593423] This study was the first to show that RAG,

upon binding a bona fide recombination signal sequence (RSS), can then linearly explore mega-base distances within convergent CTCF sites-based chromatin loop domains to identify convergently-oriented cryptic RSS targets for V(D)J recombination-based cleavage and joining, thereby providing the basis for subsequent linear RAG chromatin scanning models.

13. Dong J et al. Orientation-specific joining of AID-initiated DNA breaks promotes antibody class switching. *Nature* 525, 134–139 (2015). [PubMed: 26308889]
14. Collins PL et al. DNA double-strand breaks induce H2Ax phosphorylation domains in a contact-dependent manner. *Nat. Commun* 11, 3158 (2020). [PubMed: 32572033]
15. Arnould C et al. Loop extrusion as a mechanism for formation of DNA damage repair foci. *Nature* 590, 660–665 (2021). [PubMed: 33597753] This study provided evidence for a key role of cohesin-mediated loop extrusion in general double-strand break repair which involves facilitating the formation of long double-strand break response foci critical for double-strand break end synapsis and joining.
16. Ochs F et al. Stabilization of chromatin topology safeguards genome integrity. *Nature* 574, 571–574 (2019). [PubMed: 31645724]
17. Dekker J & Mirny L The 3D Genome as Moderator of Chromosomal Communication. *Cell* 164, 1110–1121 (2016). [PubMed: 26967279]
18. Rao SS et al. A 3D map of the human genome at kilobase resolution reveals principles of chromatin looping. *Cell* 159, 1665–1680 (2014). [PubMed: 25497547] This study is the first to report kilobase high-resolution Hi-C maps which revealed a genome-wide prevalence of convergent CTCF sites at the chromatin loop anchors, providing a key observation for the cohesin-mediated loop-extrusion model.
19. Nasmyth K Disseminating the genome: joining, resolving, and separating sister chromatids during mitosis and meiosis. *Annu. Rev. Genet* 35, 673–745 (2001). [PubMed: 11700297]
20. Alipour E & Marko JF Self-organization of domain structures by DNA-loop-extruding enzymes. *Nucleic Acids Res.* 40, 11202–11212 (2012). [PubMed: 23074191]
21. Sanborn AL et al. Chromatin extrusion explains key features of loop and domain formation in wild-type and engineered genomes. *Proc. Natl Acad. Sci. USA* 112, E6456–6465 (2015). [PubMed: 26499245] This paper, together with the study by Fudenberg et al., (ref 24), provided strong evidence to support a chromatin loop extrusion process, likely driven by cohesin, as the underlying mechanism for the formation of convergent CTCF sites-based contact loop domains.
22. Nichols MH & Corces VG A CTCF Code for 3D Genome Architecture. *Cell* 162, 703–705 (2015). [PubMed: 26276625]
23. Bouwman BA & de Laat W Getting the genome in shape: the formation of loops, domains and compartments. *Genome Biol.* 16, 154 (2015). [PubMed: 26257189]
24. Fudenberg G et al. Formation of Chromosomal Domains by Loop Extrusion. *Cell Rep.* 15, 2038–2049 (2016). [PubMed: 27210764] This paper, together with the study by Sanborn et al (ref 21), provided strong evidence to support a chromatin loop extrusion process, likely driven by cohesin, as the underlying mechanism for the formation of convergent CTCF sites-based contact loop domains.
25. Jain S, Ba Z, Zhang Y, Dai HQ & Alt FW CTCF-Binding Elements Mediate Accessibility of RAG Substrates During Chromatin Scanning. *Cell* 174, 102–116 e114 (2018). [PubMed: 29804837] This paper provided evidence that supports a model in which the Igh V(D)J recombination-centre serves as a dynamic loop anchor to allow cohesin-mediated loop extrusion to present upstream chromatin for scanning by RAG endonuclease and also demonstrated that CTCF sites promote accessibility of associated proximal VHs by increasing their interaction with the V(D)J recombination-centre during scanning.
26. Zhang Y et al. The fundamental role of chromatin loop extrusion in physiological V(D)J recombination. *Nature* 573, 600–604 (2019). [PubMed: 31511698] This paper provided evidence that loop extrusion-mediated RAG scanning is the major mechanism for physiological, deletional D-to-J_H recombination and mechanisms beyond CTCF sites-based loop anchors, including active transcription and nuclease-dead Cas9 protein binding can impede loop extrusion-mediated scanning and promote RAG targeting activity.
27. Ba Z et al. CTCF orchestrates long-range cohesin-driven V(D)J recombinational scanning. *Nature* 586, 305–310 (2020). [PubMed: 32717742] Through a targeted depletion of cohesin or CTCF in

v-Abl cell lines, this paper provided evidence that cohesin drives loop-extrusion-mediated RAG chromatin scanning and provided proof-of-principle that dampening of CTCF sites-based anchors can promote loop extrusion, locus contraction, and long-range RAG scanning.

28. Hill L et al. *Wapl* repression by Pax5 promotes V gene recombination by Igh loop extrusion. *Nature* 584, 142–147 (2020). [PubMed: 32612238] This study showed that PAX5-mediated suppression of *Wapl* transcription in pro-B cells results in global extension of chromosomal loops, which implicated loop extrusion as the long-sought mechanism for V_H locus contraction and distal V_H utilization.
29. Dai HQ et al. Loop extrusion mediates physiological Igh locus contraction for RAG scanning. *Nature* 590, 338–343 (2021). [PubMed: 33442057] By studying utilization of cryptic RSSs across normal and inverted V_H loci, this study demonstrated linear RAG scanning across the V_H locus in normal pro-B cells and also implicated WAPL down-regulation in promoting loop extrusion-mediated locus contraction and long-range RAG scanning.
30. Zhang X et al. Fundamental roles of chromatin loop extrusion in antibody class switching. *Nature* 575, 385–389 (2019). [PubMed: 31666703] This paper showed that cohesin-mediated loop extrusion plays a fundamental role in the physiological, deletional *Igh* class switch recombination (CSR) mechanism, by establishing a CSR-centre that orchestrates substrate S region activation and synapsis, as well as post-cleavage deletional joining of S region double-strand breaks.
31. Zhang X, Yoon HS, Chapdelaine-Williams AM, Kyritsis N & Alt FW Physiological role of the 3'IgH CBEs super-anchor in antibody class switching. *Proc. Natl Acad. Sci. USA* 118 (2021). This paper showed that the 3' *Igh* CTCF sites serve as an insulator to focus chromatin loop extrusion-mediated transcriptional and CSR activities within the upstream C_H-containing domain.
32. Alt FW, Zhang Y, Meng FL, Guo C & Schwer B Mechanisms of programmed DNA lesions and genomic instability in the immune system. *Cell* 152, 417–429 (2013). [PubMed: 23374339]
33. Methot SP & Di Noia JM Molecular Mechanisms of Somatic Hypermutation and Class Switch Recombination. *Adv. Immunol* 133, 37–87 (2017). [PubMed: 28215280]
34. Ong CT & Corces VG CTCF: an architectural protein bridging genome topology and function. *Nat. Rev. Genet* 15, 234–246 (2014). [PubMed: 24614316]
35. Degner SC, Wong TP, Jankevicius G & Feeney AJ Cutting edge: developmental stage-specific recruitment of cohesin to CTCF sites throughout immunoglobulin loci during B lymphocyte development. *J Immunol* 182, 44–48 (2009). [PubMed: 19109133]
36. Proudhon C, Hao B, Raviram R, Chaumeil J & Skok JA Long-Range Regulation of V(D)J Recombination. *Adv Immunol* 128, 123–182 (2015). [PubMed: 26477367]
37. MacPherson MJ & Sadowski PD The CTCF insulator protein forms an unusual DNA structure. *BMC Mol. Biol* 11, 101 (2010). [PubMed: 21176138]
38. Nakahashi H et al. A genome-wide map of CTCF multivalency redefines the CTCF code. *Cell Rep.* 3, 1678–1689 (2013). [PubMed: 23707059]
39. Vietri Rudan M et al. Comparative Hi-C reveals that CTCF underlies evolution of chromosomal domain architecture. *Cell Rep.* 10, 1297–1309 (2015). [PubMed: 25732821]
40. de Wit E et al. CTCF Binding Polarity Determines Chromatin Looping. *Mol. Cell* 60, 676–684 (2015). [PubMed: 26527277]
41. Kagey MH et al. Mediator and cohesin connect gene expression and chromatin architecture. *Nature* 467, 430–435 (2010). [PubMed: 20720539]
42. Zuin J et al. A cohesin-independent role for NIPBL at promoters provides insights in CdLS. *PLoS Genet.* 10, e1004153 (2014). [PubMed: 24550742]
43. Dorsett D & Merkenschlager M Cohesin at active genes: a unifying theme for cohesin and gene expression from model organisms to humans. *Curr. Opin. Cell Biol* 25, 327–333 (2013). [PubMed: 23465542]
44. Li Y et al. The structural basis for cohesin-CTCF-anchored loops. *Nature* 578, 472–476 (2020). [PubMed: 31905366]
45. Nishana M et al. Defining the relative and combined contribution of CTCF and CTCFL to genomic regulation. *Genome Biol.* 21, 108 (2020). [PubMed: 32393311]
46. Pugacheva EM et al. CTCF mediates chromatin looping via N-terminal domain-dependent cohesin retention. *Proc. Natl Acad. Sci. USA* 117, 2020–2031 (2020). [PubMed: 31937660]

47. Nora EP et al. Molecular basis of CTCF binding polarity in genome folding. *Nat. Commun* 11, 5612 (2020). [PubMed: 33154377]
48. Mirny L & Dekker J Mechanisms of Chromosome Folding and Nuclear Organization: Their Interplay and Open Questions. *Cold Spring Harb. Perspect. Biol* 10.1101/cshperspect.a040147 (2021).
49. Hansen AS, Pustova I, Cattoglio C, Tjian R & Darzacq X CTCF and cohesin regulate chromatin loop stability with distinct dynamics. *Elife* 6, e25776 (2017). [PubMed: 28467304]
50. Hansen AS, Cattoglio C, Darzacq X & Tjian R Recent evidence that TADs and chromatin loops are dynamic structures. *Nucleus* 9, 20–32 (2018). [PubMed: 29077530]
51. Rowley MJ & Corces VG Organizational principles of 3D genome architecture. *Nat. Rev. Genet* 19, 789–800 (2018). [PubMed: 30367165]
52. Davidson IF & Peters JM Genome folding through loop extrusion by SMC complexes. *Nat. Rev. Mol. Cell Biol* 22, 445–464 (2021). [PubMed: 33767413]
53. Lin SG, Ba Z, Alt FW & Zhang Y RAG Chromatin Scanning During V(D)J Recombination and Chromatin Loop Extrusion are Related Processes. *Adv. Immunol* 139, 93–135 (2018). [PubMed: 30249335]
54. Kraft K et al. Serial genomic inversions induce tissue-specific architectural stripes, gene misexpression and congenital malformations. *Nat. Cell Biol* 21, 305–310 (2019). [PubMed: 30742094]
55. Hsieh TS et al. Resolving the 3D Landscape of Transcription-Linked Mammalian Chromatin Folding. *Mol. Cell* 78, 539–553 e538 (2020). [PubMed: 32213323]
56. Thiecke MJ et al. Cohesin-Dependent and -Independent Mechanisms Mediate Chromosomal Contacts between Promoters and Enhancers. *Cell Rep.* 32, 107929 (2020). [PubMed: 32698000]
57. Nora EP et al. Targeted Degradation of CTCF Decouples Local Insulation of Chromosome Domains from Genomic Compartmentalization. *Cell* 169, 930–944 e922 (2017). [PubMed: 28525758]
58. Wutz G et al. Topologically associating domains and chromatin loops depend on cohesin and are regulated by CTCF, WAPL, and PDS5 proteins. *EMBO J.* 36, 3573–3599 (2017). [PubMed: 29217591] This study, together with ref 59 and ref 65, showed that depletion of WAPL, the cohesin unloading factor, increases cohesin chromatin retention time and leads to extension of chromatin loop sizes genome-wide.
59. Gassler J et al. A mechanism of cohesin-dependent loop extrusion organizes zygotic genome architecture. *EMBO J.* 36, 3600–3618 (2017). [PubMed: 29217590] This study, together with ref 58 and ref 65, showed that depletion of WAPL, the cohesin unloading factor, increases cohesin chromatin retention time and leads to extension of chromatin loop sizes genome-wide.
60. Rao SSP et al. Cohesin Loss Eliminates All Loop Domains. *Cell* 171, 305–320 e324 (2017). [PubMed: 28985562]
61. Schwarzer W et al. Two independent modes of chromatin organization revealed by cohesin removal. *Nature* 551, 51–56 (2017). [PubMed: 29094699]
62. Vian L et al. The Energetics and Physiological Impact of Cohesin Extrusion. *Cell* 173, 1165–1178 e1120 (2018). [PubMed: 29706548]
63. Gandhi R, Gillespie PJ & Hirano T Human Wapl is a cohesin-binding protein that promotes sister-chromatid resolution in mitotic prophase. *Curr. Biol* 16, 2406–2417 (2006). [PubMed: 17112726]
64. Kueng S et al. Wapl controls the dynamic association of cohesin with chromatin. *Cell* 127, 955–967 (2006). [PubMed: 17113138]
65. Haarhuis JHI et al. The Cohesin Release Factor WAPL Restricts Chromatin Loop Extension. *Cell* 169, 693–707 e614 (2017). [PubMed: 28475897] This study, together with ref 58 and ref 59, showed that depletion of WAPL, the cohesin unloading factor, increases cohesin chromatin retention time and leads to extension of chromatin loop sizes genome-wide.
66. Davidson IF et al. DNA loop extrusion by human cohesin. *Science* 366, 1338–1345 (2019). [PubMed: 31753851]
67. Kim Y, Shi Z, Zhang H, Finkelstein IJ & Yu H Human cohesin compacts DNA by loop extrusion. *Science* 366, 1345–1349 (2019). [PubMed: 31780627]

68. Golfier S, Quail T, Kimura H & Bruges J Cohesin and condensin extrude DNA loops in a cell cycle-dependent manner. *Elife* 9, e53885 (2020). [PubMed: 32396063]
69. Ribeiro de Almeida C, Hendriks RW & Stadhouders R Dynamic Control of Long-Range Genomic Interactions at the Immunoglobulin kappa Light-Chain Locus. *Adv. Immunol* 128, 183–271 (2015). [PubMed: 26477368]
70. Schatz DG & Swanson PC V(D)J recombination: mechanisms of initiation. *Annu. Rev. Genet* 45, 167–202 (2011). [PubMed: 21854230]
71. Teng G & Schatz DG Regulation and Evolution of the RAG Recombinase. *Adv Immunol* 128, 1–39 (2015). [PubMed: 26477364]
72. Jung D, Giallourakis C, Mostoslavsky R & Alt FW Mechanism and control of V(D)J recombination at the immunoglobulin heavy chain locus. *Annu. Rev. Immunol* 24, 541–570 (2006). [PubMed: 16551259]
73. Kim MS, Lapkouski M, Yang W & Gellert M Crystal structure of the V(D)J recombinase RAG1-RAG2. *Nature* 518, 507–511 (2015). [PubMed: 25707801]
74. Ru H et al. Molecular Mechanism of V(D)J Recombination from Synaptic RAG1-RAG2 Complex Structures. *Cell* 163, 1138–1152 (2015). [PubMed: 26548953]
75. Kim MS et al. Cracking the DNA Code for V(D)J Recombination. *Mol. Cell* 70, 358–370 e354 (2018). [PubMed: 29628308]
76. Ru H et al. DNA melting initiates the RAG catalytic pathway. *Nat. Struct. Mol. Biol* 25, 732–742 (2018). [PubMed: 30061602]
77. Grundy GJ et al. Initial stages of V(D)J recombination: the organization of RAG1/2 and RSS DNA in the postcleavage complex. *Mol. Cell* 35, 217–227 (2009). [PubMed: 19647518]
78. Wang XS, Lee BJ & Zha S The recent advances in non-homologous end-joining through the lens of lymphocyte development. *DNA Repair (Amst)* 94, 102874 (2020). [PubMed: 32623318]
79. Zhao B, Rothenberg E, Ramsden DA & Lieber MR The molecular basis and disease relevance of non-homologous DNA end joining. *Nat. Rev. Mol. Cell Biol* 21, 765–781 (2020). [PubMed: 33077885]
80. Ji Y et al. The in vivo pattern of binding of RAG1 and RAG2 to antigen receptor loci. *Cell* 141, 419–431 (2010). [PubMed: 20398922]
81. Teng G et al. RAG Represents a Widespread Threat to the Lymphocyte Genome. *Cell* 162 (2015).
82. Guo C et al. CTCF-binding elements mediate control of V(D)J recombination. *Nature* 477, 424–430 (2011). [PubMed: 21909113]
83. Lin SG, Guo C, Su A, Zhang Y & Alt FW CTCF-binding elements 1 and 2 in the Igh intergenic control region cooperatively regulate V(D)J recombination. *Proc. Natl Acad. Sci. USA* 112, 1815–1820 (2015). [PubMed: 25624508]
84. Garrett FE et al. Chromatin architecture near a potential 3' end of the igh locus involves modular regulation of histone modifications during B-Cell development and in vivo occupancy at CTCF sites. *Mol. Cell Biol* 25, 1511–1525 (2005). [PubMed: 15684400]
85. Degner SC et al. CCCTC-binding factor (CTCF) and cohesin influence the genomic architecture of the Igh locus and antisense transcription in pro-B cells. *Proc. Natl Acad. Sci. USA* 108, 9566–9571 (2011). [PubMed: 21606361]
86. Benner C, Isoda T & Murre C New roles for DNA cytosine modification, eRNA, anchors, and superanchors in developing B cell progenitors. *Proc. Natl Acad. Sci. USA* 112, 12776–12781 (2015). [PubMed: 26417104]
87. Aiden EL & Casellas R Somatic Rearrangement in B Cells: It's (Mostly) Nuclear Physics. *Cell* 162, 708–711 (2015). [PubMed: 26276627]
88. Kosak ST et al. Subnuclear compartmentalization of immunoglobulin loci during lymphocyte development. *Science* 296, 158–162 (2002). [PubMed: 11935030]
89. Fuxa M et al. Pax5 induces V-to-DJ rearrangements and locus contraction of the immunoglobulin heavy-chain gene. *Genes Dev* 18, 411–422 (2004). [PubMed: 15004008]
90. Sayegh CE, Jhunjhunwala S, Riblet R & Murre C Visualization of looping involving the immunoglobulin heavy-chain locus in developing B cells. *Genes Dev.* 19, 322–327 (2005). [PubMed: 15687256]

91. Roldan E et al. Locus 'decontraction' and centromeric recruitment contribute to allelic exclusion of the immunoglobulin heavy-chain gene. *Nat. Immunol* 6, 31–41 (2005). [PubMed: 15580273]
92. Jhunjhunwala S et al. The 3D structure of the immunoglobulin heavy-chain locus: implications for long-range genomic interactions. *Cell* 133, 265–279 (2008). [PubMed: 18423198]
93. Medvedovic J et al. Flexible long-range loops in the VH gene region of the Igh locus facilitate the generation of a diverse antibody repertoire. *Immunity* 39, 229–244 (2013). [PubMed: 23973221]
94. Rother MB et al. Nuclear positioning rather than contraction controls ordered rearrangements of immunoglobulin loci. *Nucleic Acids Res.* 44, 175–186 (2016). [PubMed: 26384565]
95. Montefiori L et al. Extremely Long-Range Chromatin Loops Link Topological Domains to Facilitate a Diverse Antibody Repertoire. *Cell Rep.* 14, 896–906 (2016). [PubMed: 26804913]
96. Bossen C, Mansson R & Murre C Chromatin topology and the regulation of antigen receptor assembly. *Annu. Rev. Immunol* 30, 337–356 (2012). [PubMed: 22224771]
97. Ebert A, Hill L & Busslinger M Spatial Regulation of V-(D)J Recombination at Antigen Receptor Loci. *Adv. Immunol* 128, 93–121 (2015). [PubMed: 26477366]
98. Rogers CH, Mielczarek O & Corcoran AE Dynamic 3D Locus Organization and Its Drivers Underpin Immunoglobulin Recombination. *Front. Immunol* 11, 633705 (2020). [PubMed: 33679727]
99. Lucas JS, Zhang Y, Dudko OK & Murre C 3D trajectories adopted by coding and regulatory DNA elements: first-passage times for genomic interactions. *Cell* 158, 339–352 (2014). [PubMed: 24998931]
100. Ranganath S et al. Productive coupling of accessible Vbeta14 segments and DJbeta complexes determines the frequency of Vbeta14 rearrangement. *J. Immunol* 180, 2339–2346 (2008). [PubMed: 18250443]
101. Helmink BA & Sleckman BP The response to and repair of RAG-mediated DNA double-strand breaks. *Annu. Rev. Immunol.* 30, 175–202 (2012). [PubMed: 22224778]
102. Nussenzweig A & Nussenzweig MC Origin of chromosomal translocations in lymphoid cancer. *Cell* 141, 27–38 (2010). [PubMed: 20371343]
103. Tepsuporn S, Hu J, Gostissa M & Alt FW Mechanisms that can promote peripheral B-cell lymphoma in ATM-deficient mice. *Cancer Immunol. Res* 2, 857–866 (2014). [PubMed: 24913718]
104. Bredemeyer AL et al. ATM stabilizes DNA double-strand-break complexes during V(D)J recombination. *Nature* 442, 466–470 (2006). [PubMed: 16799570]
105. Wood C & Tonegawa S Diversity and joining segments of mouse immunoglobulin heavy chain genes are closely linked and in the same orientation: implications for the joining mechanism. *Proc Natl Acad Sci U S A* 80, 3030–3034, doi:10.1073/pnas.80.10.3030 (1983). [PubMed: 6407007]
106. Yancopoulos GD et al. Preferential utilization of the most JH-proximal VH gene segments in pre-B-cell lines. *Nature* 311, 727–733 (1984). [PubMed: 6092962]
107. Gauss GH & Lieber MR The basis for the mechanistic bias for deletional over inversional V(D)J recombination. *Genes Dev.* 6, 1553–1561 (1992). [PubMed: 1644296]
108. Choi NM et al. Deep sequencing of the murine IgH repertoire reveals complex regulation of nonrandom V gene rearrangement frequencies. *J. Immunol* 191, 2393–2402 (2013). [PubMed: 23898036]
109. Bolland DJ et al. Two Mutually Exclusive Local Chromatin States Drive Efficient V(D)J Recombination. *Cell Rep.* 15, 2475–2487.
110. Khanna N, Zhang Y, Lucas JS, Dudko OK & Murre C Chromosome dynamics near the sol-gel phase transition dictate the timing of remote genomic interactions. *Nat. Commun* 10, 2771 (2019). [PubMed: 31235807]
111. Ebert A et al. The distal V(H) gene cluster of the Igh locus contains distinct regulatory elements with Pax5 transcription factor-dependent activity in pro-B cells. *Immunity* 34, 175–187 (2011). [PubMed: 21349430]
112. Verma-Gaur J et al. Noncoding transcription within the Igh distal V(H) region at PAIR elements affects the 3D structure of the Igh locus in pro-B cells. *Proc. Natl Acad. Sci. USA* 109, 17004–17009 (2012). [PubMed: 23027941]

113. Hesslein DG et al. Pax5 is required for recombination of transcribed, acetylated, 5' IgH V gene segments. *Genes Dev.* 17, 37–42 (2003). [PubMed: 12514097]
114. Yancopoulos GD & Alt FW Developmentally controlled and tissue-specific expression of unrearranged VH gene segments. *Cell* 40, 271–281 (1985). [PubMed: 2578321]
115. Yancopoulos GD, Blackwell TK, Suh H, Hood L & Alt FW Introduced T cell receptor variable region gene segments recombine in pre-B cells: evidence that B and T cells use a common recombinase. *Cell* 44 251–259 (1986). [PubMed: 3484682]
116. Bolland DJ et al. Antisense intergenic transcription in V(D)J recombination. *Nat. Immunol* 5, 630–637 (2004). [PubMed: 15107847]
117. Bolland DJ et al. Antisense intergenic transcription precedes Igh D-to-J recombination and is controlled by the intronic enhancer *Emu*. *Mol. Cell Biol* 27, 5523–5533 (2007). [PubMed: 17526723]
118. Beilinson HA et al. The RAG1 N-terminal region regulates the efficiency and pathways of synapsis for V(D)J recombination. *J. Exp. Med* 218 e20210250 (2021). [PubMed: 34402853]
119. Qiu X et al. Sequential Enhancer Sequestration Dysregulates Recombination Center Formation at the IgH Locus. *Mol Cell* 70, 21–33 e26, doi:10.1016/j.molcel.2018.02.020 (2018). [PubMed: 29576529]
120. Chakraborty T et al. Repeat organization and epigenetic regulation of the DH-Cmu domain of the immunoglobulin heavy-chain gene locus. *Mol. Cell* 27, 842–850 (2007). [PubMed: 17803947]
121. Hwang JK, Alt FW & Yeap LS Related Mechanisms of Antibody Somatic Hypermutation and Class Switch Recombination. *Microbiol. Spectr* 3, MDNA3-0037-2014 (2015).
122. Muramatsu M et al. Class switch recombination and hypermutation require activation-induced cytidine deaminase (AID), a potential RNA editing enzyme. *Cell* 102, 553–563 (2000). [PubMed: 11007474]
123. Yeap LS & Meng FL Cis- and trans-factors affecting AID targeting and mutagenic outcomes in antibody diversification. *Adv. Immunol* 141, 51–103 (2019). [PubMed: 30904133]
124. Cascalho M, Wong J, Steinberg C & Wabl M Mismatch repair co-opted by hypermutation. *Science* 279, 1207–1210 (1998). [PubMed: 9469811]
125. Bottaro A et al. Deletion of the IgH intronic enhancer and associated matrix-attachment regions decreases, but does not abolish, class switching at the mu locus. *Int. Immunol* 10, 799–806 (1998). [PubMed: 9678761]
126. Sakai E, Bottaro A & Alt FW The Ig heavy chain intronic enhancer core region is necessary and sufficient to promote efficient class switch recombination. *Int. Immunol* 11, 1709–1713 (1999). [PubMed: 10508189]
127. Perlot T, Alt FW, Bassing CH, Suh H & Pinaud E Elucidation of IgH intronic enhancer functions via germ-line deletion. *Proc. Natl Acad. Sci. USA* 102, 14362–14367 (2005). [PubMed: 16186486]
128. Li F, Yan Y, Pieretti J, Feldman DA & Eckhardt LA Comparison of identical and functional Igh alleles reveals a nonessential role for *Emu* in somatic hypermutation and class-switch recombination. *J. Immunol* 185, 6049–6057 (2010). [PubMed: 20937850]
129. Vincent-Fabert C et al. Genomic deletion of the whole IgH 3' regulatory region (hs3a, hs1,2, hs3b, and hs4) dramatically affects class switch recombination and Ig secretion to all isotypes. *Blood* 116, 1895–1898 (2010). [PubMed: 20538806]
130. Saintamand A et al. Deciphering the importance of the palindromic architecture of the immunoglobulin heavy-chain 3' regulatory region. *Nat. Commun* 7, 10730 (2016). [PubMed: 26883548]
131. Pinaud E et al. Localization of the 3' IgH locus elements that effect long-distance regulation of class switch recombination. *Immunity* 15, 187–199 (2001). [PubMed: 11520455]
132. Wuerffel R et al. S-S synapsis during class switch recombination is promoted by distantly located transcriptional elements and activation-induced deaminase. *Immunity* 27, 711–722 (2007). [PubMed: 17980632]
133. Seidl KJ et al. Position-dependent inhibition of class-switch recombination by PGK-neo cassettes inserted into the immunoglobulin heavy chain constant region locus. *Proc. Natl Acad. Sci. USA* 96, 3000–3005 (1999). [PubMed: 10077626]

134. Harriman W, Volk H, Defranoux N & Wabl M Immunoglobulin class switch recombination. *Annu. Rev. Immunol* 11, 361–384 (1993). [PubMed: 8476566]
135. Chiarle R et al. Genome-wide translocation sequencing reveals mechanisms of chromosome breaks and rearrangements in B cells. *Cell* 147, 107–119 (2011). [PubMed: 21962511]
136. Frock RL et al. Genome-wide detection of DNA double-stranded breaks induced by engineered nucleases. *Nat. Biotechnol* 33, 179–186 (2015). [PubMed: 25503383]
137. Wei PC et al. Long Neural Genes Harbor Recurrent DNA Break Clusters in Neural Stem/Progenitor Cells. *Cell* 164, 644–655 (2016). [PubMed: 26871630]
138. Dudley DD et al. Internal IgH class switch region deletions are position-independent and enhanced by AID expression. *Proc. Natl Acad. Sci. USA* 99, 9984–9989 (2002). [PubMed: 12114543]
139. Zhao Y, Rabbani H, Shimizu A & Hammarstrom L Mapping of the chicken immunoglobulin heavy-chain constant region gene locus reveals an inverted alpha gene upstream of a condensed epsilon gene. *Immunology* 101, 348–353 (2000). [PubMed: 11106938]
140. Lundqvist ML, Middleton DL, Hazard S & Warr GW The immunoglobulin heavy chain locus of the duck. Genomic organization and expression of D, J, and C region genes. *J. Biol. Chem* 276, 46729–46736 (2001). [PubMed: 11592961]
141. Xiong H, Dolpady J, Wabl M, Curotto de Lafaille MA & Lafaille JJ Sequential class switching is required for the generation of high affinity IgE antibodies. *J. Exp. Med* 209, 353–364 (2012). [PubMed: 22249450]
142. Mandler R, Finkelman FD, Levine AD & Snapper CM IL-4 induction of IgE class switching by lipopolysaccharide-activated murine B cells occurs predominantly through sequential switching. *J. Immunol* 150, 407–418 (1993). [PubMed: 8419474]
143. Zhang T et al. Downstream class switching leads to IgE antibody production by B lymphocytes lacking IgM switch regions. *Proc. Natl Acad. Sci. USA* 107, 3040–3045 (2010). [PubMed: 20133637]
144. Yu K An insulator that regulates chromatin extrusion and class switch recombination. *Proc. Natl Acad. Sci. USA* 118, e2026399118 (2021). [PubMed: 33479168]
145. Bassing CH & Alt FW The cellular response to general and programmed DNA double strand breaks. *DNA Repair (Amst)* 3, 781–796, doi:10.1016/j.dnarep.2004.06.001 (2004). [PubMed: 15279764]
146. Liu Y et al. Very fast CRISPR on demand. *Science* 368, 1265–1269 (2020). [PubMed: 32527834]
147. Li K, Bronk G, Kondev J & Haber JE Yeast ATM and ATR kinases use different mechanisms to spread histone H2A phosphorylation around a DNA double-strand break. *Proc. Natl Acad. Sci. USA* 117, 21354–21363 (2020). [PubMed: 32817543]
148. Mirny LA Cells use loop extrusion to weave and tie the genome. *Nature* 590, 554–555 (2021). [PubMed: 33597775]
149. Desiderio S Temporal and spatial regulatory functions of the V(D)J recombinase. *Semin. Immunol* 22, 362–369 (2010). [PubMed: 21036059]
150. Majumder K, Bassing CH & Oltz EM Regulation of Tcrb Gene Assembly by Genetic, Epigenetic, and Topological Mechanisms. *Adv. Immunol* 128, 273–306 (2015). [PubMed: 26477369]
151. Carico Z & Krangel MS Chromatin Dynamics and the Development of the TCRalpha and TCRdelta Repertoires. *Adv. Immunol* 128, 307–361 (2015). [PubMed: 26477370]
152. Fischer C et al. Conservation of the T-cell receptor alpha/delta linkage in the teleost fish *Tetraodon nigroviridis*. *Genomics* 79, 241–248 (2002). [PubMed: 11829494]
153. Fitzsimmons SP, Bernstein RM, Max EE, Skok JA & Shapiro MA Dynamic changes in accessibility, nuclear positioning, recombination, and transcription at the Ig kappa locus. *J. Immunol* 179, 5264–5273 (2007). [PubMed: 17911612]
154. Ribeiro de Almeida C et al. The DNA-binding protein CTCF limits proximal V kappa recombination and restricts kappa enhancer interactions to the immunoglobulin kappa light chain locus. *Immunity* 35, 501–513 (2011). [PubMed: 22035845]
155. Stadhouders R et al. Pre-B cell receptor signaling induces immunoglobulin kappa locus accessibility by functional redistribution of enhancer-mediated chromatin interactions. *PLoS Biol.* 12, e1001791 (2014). [PubMed: 24558349]

156. Lin YC et al. Global changes in the nuclear positioning of genes and intra- and interdomain genomic interactions that orchestrate B cell fate. *Nat. Immunol* 13, 1196–1204 (2012). [PubMed: 23064439]
157. Xiang Y, Park SK & Garrard WT V kappa gene repertoire and locus contraction are specified by critical DNase I hypersensitive sites within the V kappa-J kappa intervening region. *J. Immunol* 190, 1819–1826 (2013). [PubMed: 23296705]
158. Liu Z et al. A recombination silencer that specifies heterochromatin positioning and ikaros association in the immunoglobulin kappa locus. *Immunity* 24, 405–415 (2006). [PubMed: 16618599]
159. Xiang Y, Zhou X, Hewitt SL, Skok JA & Garrard WT A multifunctional element in the mouse Ig kappa locus that specifies repertoire and Ig loci subnuclear location. *J. Immunol* 186, 5356–5366 (2011). [PubMed: 21441452]

Box 1:**Programmed inversional V(D)J recombination**

RSSs and cryptic RSSs located in close linear proximity to V(D)J recombination-centres can gain inversional access to RAG by a short-range diffusional mechanism^{12,26}. This mechanism also may explain inversional V joining at T cell receptor- β ¹⁵⁰ and T cell receptor- δ ¹⁵¹ loci. Both loci mainly undergo deletional V(D)J recombination, but contain a single V segment in close proximity to the V(D)J recombination-centre that undergoes inversional joining. Similar mechanisms could explain inversional joining in the highly compact teleost T cell receptor- α/δ locus^{151,152}. However, long-range inversional V(D)J recombination in the *Ig κ* locus must involve distinct mechanisms. The 3.2 Mb *Ig κ* locus, which is subject to locus contraction^{91,94,153-156}, undergoes V κ -to-J κ rearrangement between 92 functional V κ segments and 4 J κ segments^{36,69}. Whereas the proximal and distal V κ segments are oriented for deletional joining to J κ , the middle V κ segments are mostly oriented for inversional joining⁶⁹. The short V κ -J κ intergenic region contains Cer¹⁵⁷ and Sis¹⁵⁸ elements containing CTCF sites. Deletion of either Cer or Sis increases the use of proximal V κ segments and decreases the use of distal V κ segments^{157,159}, which is reminiscent of the effects of IGCR1 deletion in the *Igh* locus⁸². However, long-range inversional joining of distant middle V κ segments to J κ segments is not consistent with direct linear RAG scanning. In theory, *Ig κ* may be structurally optimized for the mechanisms described above for low-level inverted D-to-J_H joining²⁶ or incorporate proximity mediated by phase separation [G]¹¹⁰. Such mechanisms could, in theory, bring V κ RSSs close enough to the J κ -V(D)J recombination-centre for a short-range diffusion-mediated joining. Although a role for cohesin-mediated loop extrusion in *Ig κ* locus contraction seems likely, it has not been tested. Targeted deletions and inversions of *Ig κ* domains and the use of high-resolution approaches to address cryptic RSS use across *Ig κ* could, as shown for *Igh*, provide more mechanistic insights.

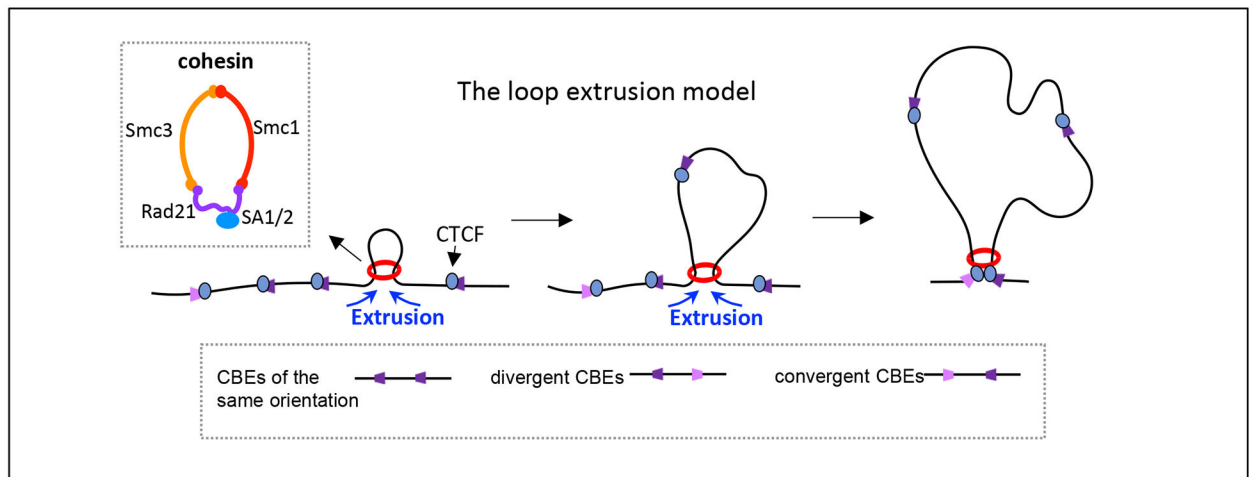


Figure 1 |. The loop extrusion model.

A simplified version of the loop extrusion model is outlined (adapted with permission from REF. 53). The extrusion model suggests that progressive extrusion of chromatin by the cohesin complex (red ring) leads to the formation of chromatin loops anchored by the structural protein CTCF (CCCTC-binding factor) bound to convergent CTCF sites. CTCF sites can be found in the genome in three orientations relative to each other (same, divergent and convergent). The inset box shows a schematic of the highly conserved cohesin ring-shaped protein complex, which is composed of the core subunits SMC1, SMC3 and RAD21 associated with either SA1 or SA2 in somatic cells.

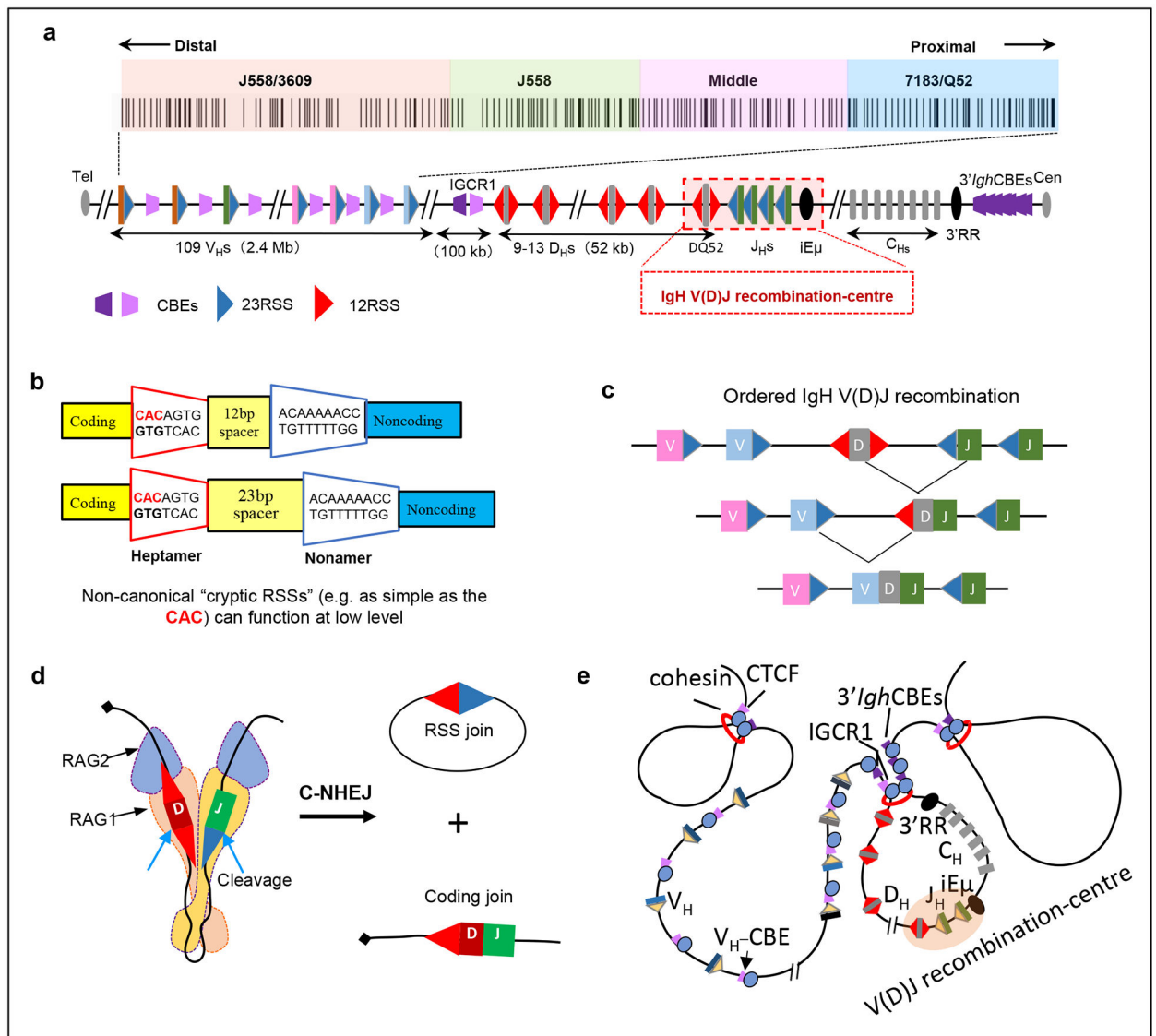


Figure 2 | The *Igh* locus initiates V(D)J recombination at the V(D)J recombination-centre.

a | The mouse 2.8 Mb immunoglobulin heavy chain (*Igh*) locus. Upstream of the *Igh* constant region exon (C_H)-containing domain, there is a 3 kb region containing the intronic *Igh* enhancer (iEμ), 4 J_H segments (J_H) and the D segment DQ52, which binds RAG to form the J_H-based V(D)J recombination-centre. Upstream of the V(D)J recombination-centre is a 52 kb region containing 9–14 D segments, an approximately 100 kb intervening region containing intergenic control region 1 (IGCR1), and the 2.4 Mb V_H-containing telomeric region (locus not drawn to scale). The V_H portion of the *Igh* locus consists of approximately 100 V_H segments clustered into four general groups that are specified by V_H family type and position; from proximal to distal location these are V_H7183/V_HQ52, middle V_Hs without a specific family type, V_HJ558 and V_HJ558/V_H3609. The four V_H groups are colour-coded, which is maintained in subsequent figures. The position and orientation of CTCF-binding sites, as well as of recombination signal sequences (12-RSSs and 23-RSSs) are shown. 12-RSSs are located upstream and downstream of D segments, 23-RSSs are

located upstream of J_{H^S} and downstream of V_{H^S} . **3' *Igh*RR**, 3' IgH regulatory region **b** | Sequence organization of bona fide 12-RSSs and 23-RSSs. The first three nucleotides (CAC) of the heptamer define the cleavage site for RAG endonuclease (RAG1–RAG2) and are crucial for RSS functionality. Cryptic RSSs as simple as CAC can be cleaved by RAG at low levels. **c** | *Igh* recombination occurs in an ordered manner, with D-to- J_H joining preceding V_H -to- DJ_H joining. **d** | RAG is recruited to the V(D)J recombination-centre, where it binds a J_H 23-RSS paired with a D_H 12-RSS and aligns them for 12/23-restricted cleavage, with the ends being joined by classical non-homologous end joining (C-NHEJ). **e** | Illustration of *Igh* domain organization showing that D_{H^S} , the V(D)J recombination-centre and C_{H^S} are contained within a 3' loop domain bounded by IGCR1 and 3' *Igh* CTCF sites. The V_{H^S} are located within the upstream 5' region and are excluded from the D- J_H domain loop at the D-to- J_H recombination stage. The structural protein CTCF binds CTCF sites and cohesin accumulates at these sites.

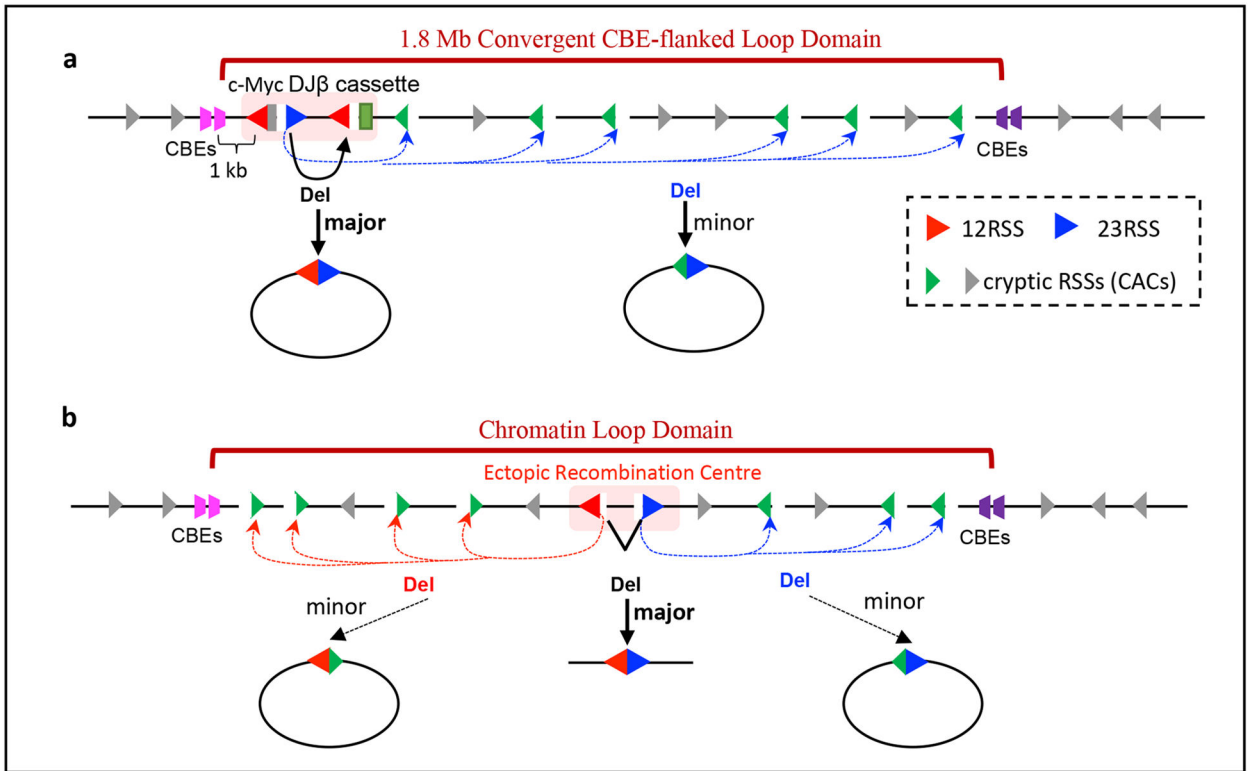


Figure 3 | Discovery of RAG long-range chromatin scanning.

a | Illustration of RAG activity initiated from bona fide D and Jβ recombination signal sequences (RSSs) in the *Myc*-DJ cassette, which, in addition to normal deletional D-to-Jβ joining within the cassette, also results in low-level joining of bona fide RSSs to hundreds of convergent cryptic RSSs across the 1.8 Mb loop domain of *Myc*¹². Cryptic RSSs in the same orientation as the *Myc*-DJ cassette generally are not used for such cryptic V(D)J recombination events. **b** | Ectopic insertion of pairs of bona fide RSSs randomly into 12 other chromatin loop domains across the genome that are known to be based on convergent CTCF sites activates RAG scanning across these loop domains¹². The orientation of the initial RAG-binding RSS prescribes the direction of RAG scanning (upstream or downstream), which continues until terminated by a loop anchor determined by convergent CTCF sites.

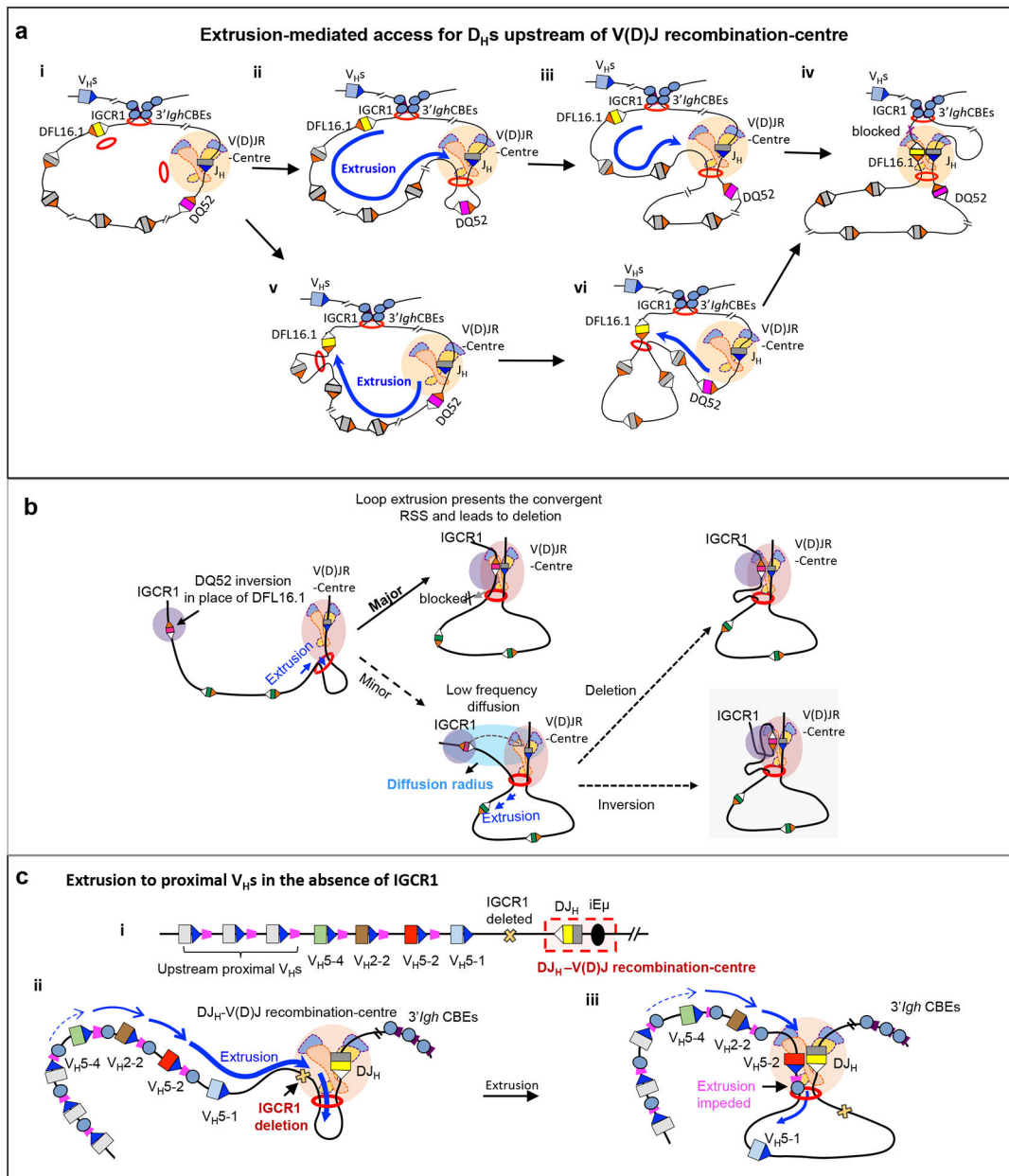


Figure 4 | Loop extrusion-mediated RAG scanning drives D-to-J_H and proximal V_H-to-DJ_H recombination.

a | Extrusion-mediated D-to-J_H recombination for D segments upstream of DQ52 and the V(D)J recombination-centre. D-to-J_H recombination occurs within the 3' *Igh* loop domain that is anchored by IGCR1 and the 3' *Igh* CTCF sites. Cohesin is known to load near the V(D)J recombination-centre²⁶ to initiate loop extrusion, but likely also at low levels at other sites such as within the D region (**part i**). The V(D)J recombination-centre functions as a broad and dynamic sub-loop anchor²⁵ (within the 3' *Igh* loop domain) that promotes cohesin-mediated loop extrusion of upstream chromatin past a RAG-bound J_H recombination signal sequence (RSS) in the V(D)J recombination-centre (**parts ii,iii**). This linear process aligns 12-RSSs downstream of D segments with the convergent RAG-bound

J_H 23-RSS for deletional D-to- J_H recombination. 12-RSSs upstream of D segments are not used for recombination owing to being in the same orientation as the J_H RSS. D segments upstream of DQ52 are frequently passed without being used for recombination, allowing loop extrusion-mediated RAG scanning to continue in many pro-B cells. Loop extrusion is strongly impeded by the IGCR1 anchor of the 3' *Igh* loop, which lies just upstream of the distal D segment DFL16.1 (**part iv**). See also Supplementary Video 1. Upon cohesin loading near DFL16.1, continuous linear extrusion brings the downstream 12-RSS of DFL16.1 to the RAG-bound J_H 23-RSS in the recombination centre. The dynamic anchor of the V(D)J recombination-centre impedes further extrusion and promotes DFL16.1 recombination (**parts v,vi**). **b** | Model of short-range diffusion-mediated inversional joining of distal D segments. Whereas loop extrusion-mediated RAG scanning drives dominant deletional joining of distal D segments, low-level inversional D joining occurs via short-range diffusion after loop extrusion brings the D segment into a 'diffusion radius' of the RAG-bound V(D)J recombination-centre. Such inversional joining is augmented by strong upstream 12-RSSs of D segments, as exemplified here by the normally dominant downstream RSS of DQ52 being placed upstream as a result of inversion of DQ52 in the DFL16.1 position. Reproduced with permission from REF. 26. **c** | Schematic of the DJ_H -V(D)J recombination-centre including its 12-RSS (white), and proximal V_H segments including their 23-RSSs and associated CTCF sites (**part i**). Upon deletion of IGCR1 or mutation of its CTCF sites, robust RAG scanning activity is extended into the proximal V_H region (**part ii**). V_{H5-2} is dominantly rearranged owing to it being the first V_H segment that is associated with a CTCF site (which impedes further loop extrusion) to be encountered during RAG scanning; the most D-proximal V_H segment V_{H5-1} lacks a functional CTCF site and is mostly bypassed without rearrangement (**part iii**). Mutation (to inactivate CTCF binding) or deletion of the V_{H5-2} CTCF site abolishes V_{H5-2} usage, rendering the next V_H segment that is flanked by a CTCF site (V_{H2-2}) as the most frequently used. Restoring the functionality of the inactive CTCF site of V_{H5-1} makes it the most frequently used V_H segment. In each case, the first several proximal V_H segments flanked by CTCF sites are used for V_H -to- DJ_H joining but at progressively reduced levels, with RAG scanning further upstream ultimately being terminated in this proximal V_H region. Parts **a** and **c** are adapted with permission from REF. 53.

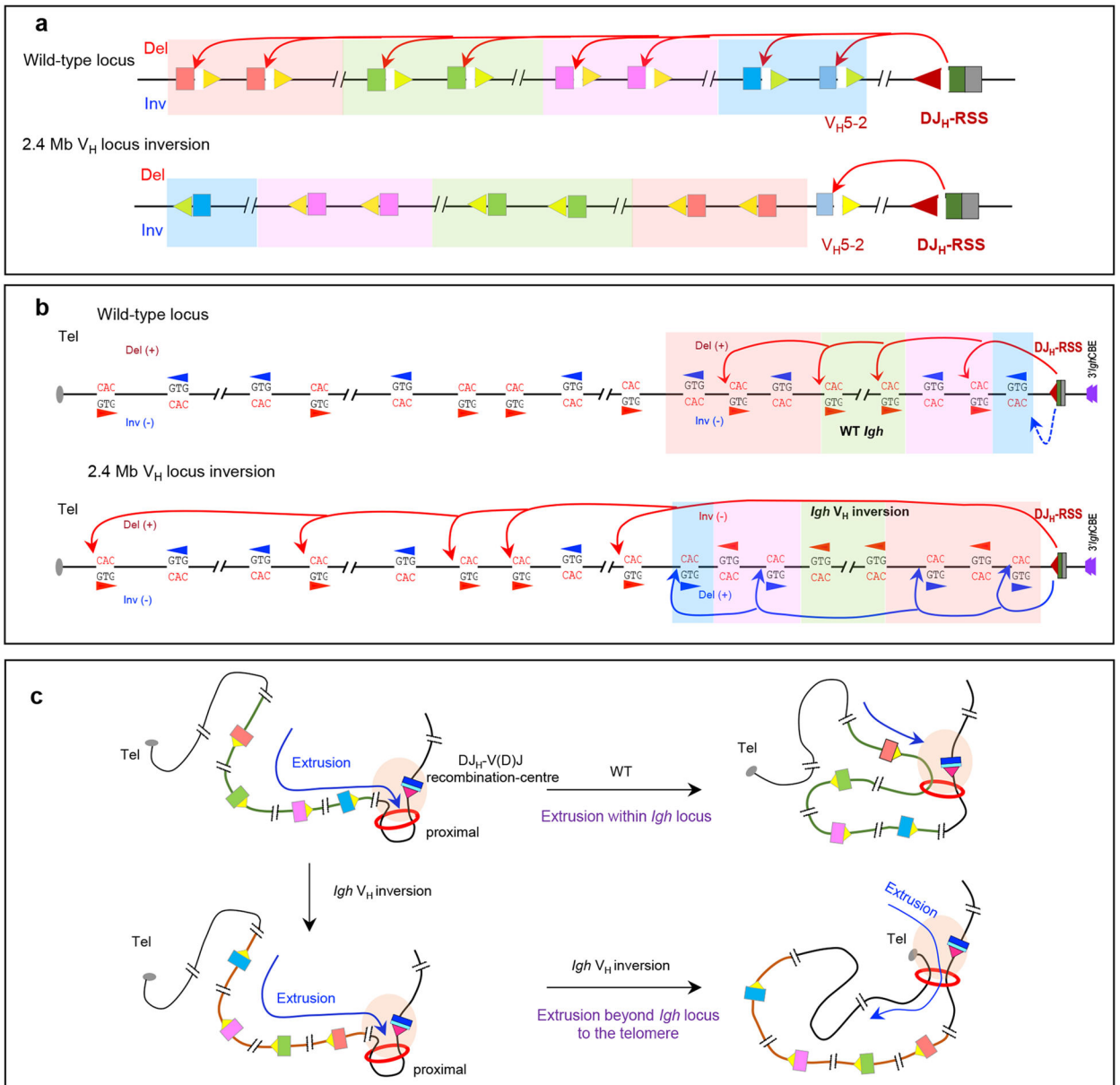


Figure 5 | Long-range RAG scanning mediates V_H use across the *Igh* locus.

a | V_H recombination signal sequences (RSSs) are all convergently oriented with respect to the DJ_H-V(D)J recombination-centre RSS, which prescribes that V_H-to-DJ_H recombination is exclusively deletional in wild-type pro-B cells. A 2.4 Mb inversion of the V_H locus spanning all V_H segments except for proximal V_H5-2 abolished the use of all inverted V_H segments in bone-marrow pro-B cells and WAPL-downregulated *v-Ab1* cell lines. **b** | RAG scanning through the V_H locus uses hundreds of cryptic RSSs (which can be as simple as the sequence CAC) in convergent orientation with the RSS of the DJ_H-V(D)J recombination-centre, with scanning terminated within the V_H locus. RAG scanning across the wild-type V_H locus would be expected often to be terminated within the V_H locus by dominant deletional rearrangements mediated by convergent V_H RSSs and DJ_H-V(D)J recombination-centre RSSs²⁹. Upon inversion of the 2.4 Mb V_H locus in primary pro-B

cells, use of cryptic RSSs normally in the convergent orientation is abrogated, whereas use of cryptic RSSs normally in the opposite orientation is activated. Inversion of the locus would eliminate the dominant deletional rearrangements in the wild-type locus, which could allow for some RAG scanning to proceed through the V_H locus. Remarkably, RAG scanning from the DJ_H - $V(D)J$ recombination-centre continued upstream of the V_H locus all the way to the telomere, targeting normally oriented cryptic RSSs within multiple, consecutive convergent loop domains beyond the *Igh* domain. This finding indicated that loop anchor impediments to scanning are likely broadly dampened in pro-B cells²⁹. Adapted with permission from REF. 29. **c** | Model for RAG scanning activity initiated by the DJ_H - $V(D)J$ recombination-centre RSS with a wild-type V_H locus or inverted V_H locus, which illustrates the findings described in panels **a** and **b**.

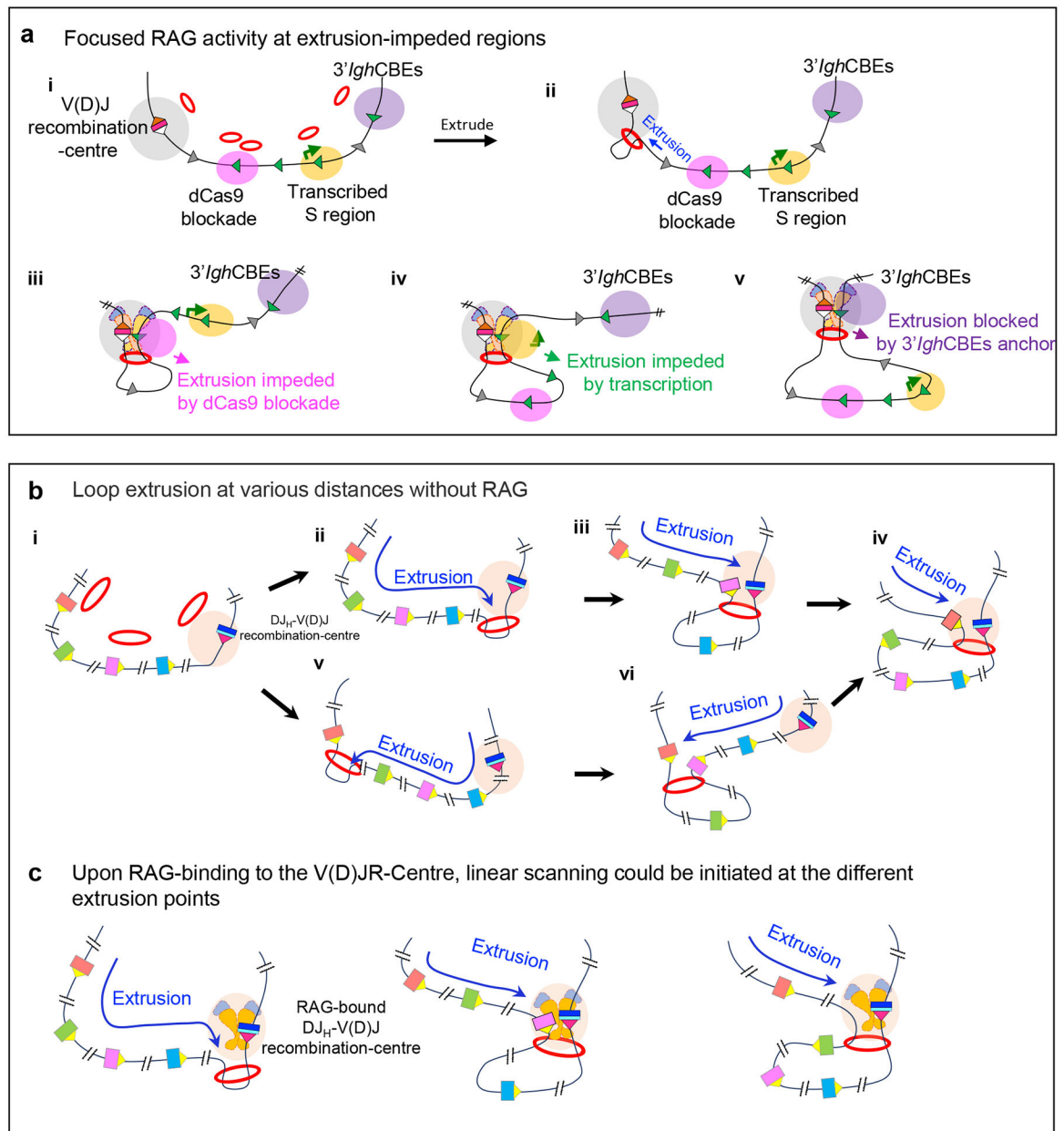


Figure 6 | Potential substrate accessibility and distal RAG scanning mechanisms in the VH locus.

a | Mechanisms that promote the targeting of cryptic recombination signal sequences (RSSs) during RAG scanning. Cohesin loaded to chromatin (multiple potential loading sites are shown) extrudes chromatin to promote interaction of the *Igh* V(D)J recombination-centre with downstream chromatin regions (**part i, ii**). The RAG-bound V(D)J recombination-centre initiates RAG scanning that can be impeded by various impediments on the scanning path, including targeted blockade by binding of catalytically ‘dead’ Cas9 (**part iii**), active transcription (**part iv**) and CTCF site-based loop anchors (**part v**). **b |** Model of loop extrusion-mediated locus contraction in the absence of RAG binding. Multiple potential cohesin loading sites are indicated. Loop extrusion theoretically could initiate from any

of these sites. Loop extrusion from a non-RAG bound, nascent $DJ_H V(D)J$ recombination-centre promotes long-range interactions with the $V(D)J$ recombination-centre to mediate *Igh* locus contraction. Extrusion is proposed to proceed over varied upstream chromatin distances in different pro-B cells prior to RAG binding. Loop extrusion might also initiate from cohesin loaded within the V_H locus. **c** | Model for use of distal V_H segments promoted by RAG binding to nascent $V(D)J$ recombination-centres. RAG binding to the $V(D)J$ recombination-centre subsequent to loop extrusion forms an active $DJ_H-V(D)J$ recombination-centre, which initiates extrusion-mediated scanning at multiple different extrusion points initiated by multiple cohesin loading points across the V_H locus. Such scanning from a variety of extrusion intermediates avoids biasing V_H recombination to the very proximal segments and thus helps to balance the primary V_H repertoire. Part **a** is adapted with permission from REF. 26. Parts **b** and **c** are adapted with permission from REF. 29.

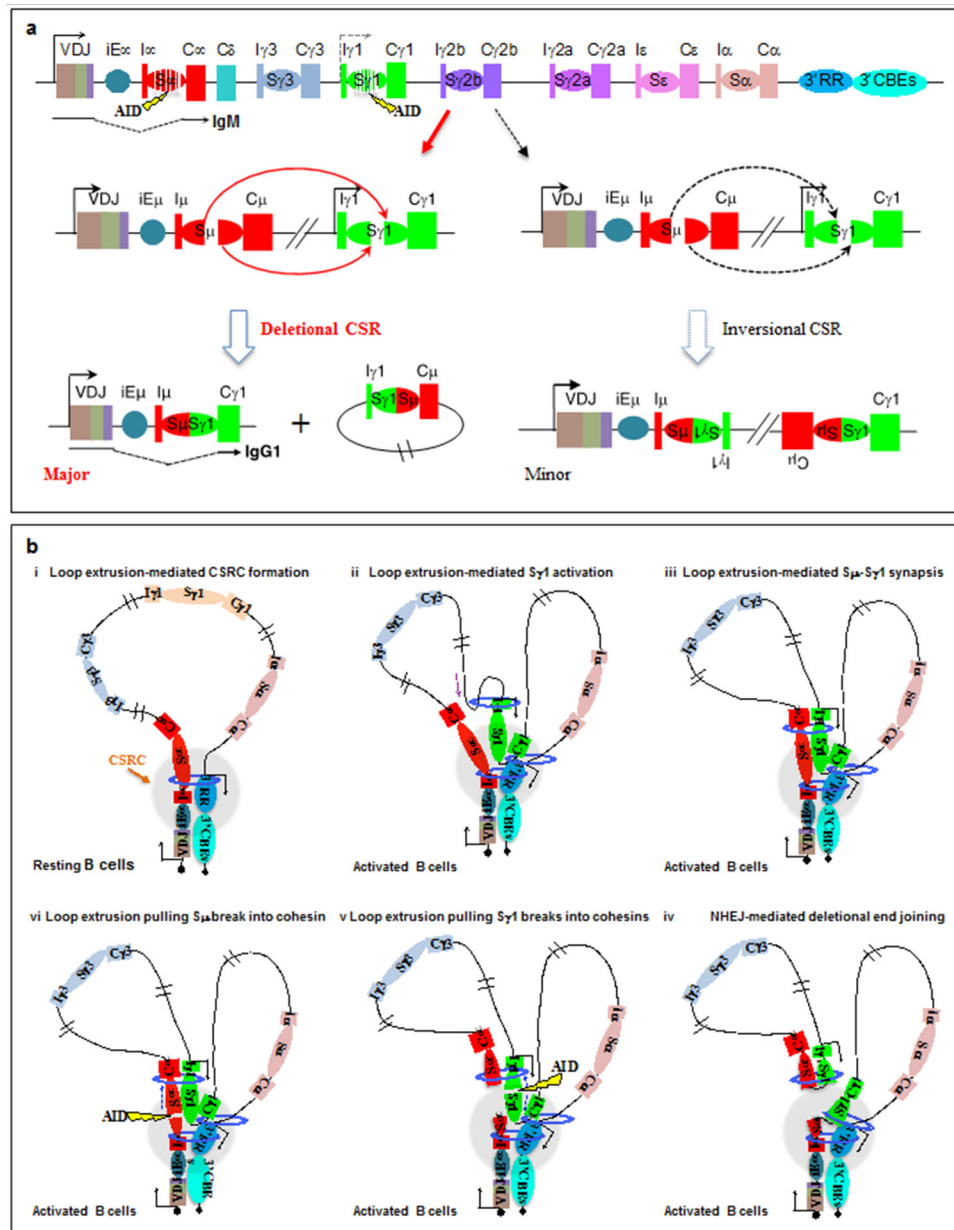


Figure 7 | Loop extrusion mediates physiological, deletional class-switch recombination.
a | Schematic of the 200 kb C_H region of the immunoglobulin heavy chain (*Igh*) locus, including the V(D)J exon, the intronic *Igh* enhancer iE_μ , the various C_H exons with inducible (I) exon and promoter upstream of each C_H segment, S regions, the 3' *Igh* regulatory region (3' *Igh*RR) super-enhancer and the 3' *Igh* CTCF sites. AID-initiated breaks within S_μ and an activated target $S_{\gamma 1}$ are illustrated, which can lead to deletional or inversional class-switch recombination (CSR) outcomes for S_μ to $S_{\gamma 1}$ joining. Deletional CSR is the major physiological event, whereas inversional CSR occurs at a lower frequency. Part **a** is adapted with permission from REF. 13. **b** | Loop extrusion mediates formation of a class-switch recombination-centre (CSR-centre) and promotes the synapsis of S region double-strand break ends for deletional joining. In resting B cells (**part i**), cohesin is

loaded at 3' *Igh*RR or iE μ -S μ and then extrudes the 3' *Igh*RR and iE μ -S μ into proximity to generate a dynamic CSR-centre. In activated B cells (**part ii**), a primed S-C_H unit (S γ 1-C γ 1 is shown as an example) is extruded to the CSR-centre for transcriptional activation and cohesin loading, which leads to further extrusion to align acceptor and donor S regions (**part iii**). Tension pulls S region double-strand break ends initiated by AID into opposing cohesin rings (**parts iv and v**), stalling extrusion and aligning them for deletional joining mediated by non-homologous end joining (NHEJ) (**part vi**). Part **b** is adapted with permission from REF. 30. See also Supplementary Video 2.